GEOLOGICA CARPATHICA, FEBRUARY 2018, 69, 1, 89–113 doi: 10.1515/geoca-2018-0006

Lower Badenian coarse-grained Gilbert deltas in the southern margin of the Western Carpathian Foredeep basin

SLAVOMÍR NEHYBA

Institute of Geological Sciences, Faculty of Science, Masaryk University, Kotlářská 2, 611 37 Brno, Czech Republic; slavek@sci.muni.cz

(Manuscript received May 15, 2017; accepted in revised form December 12, 2017)

Abstract: Two coarse-grained Gilbert-type deltas in the Lower Badenian deposits along the southern margin of the Western Carpathian Foredeep (peripheral foreland basin) were newly interpreted. Facies characterizing a range of depositional processes are assigned to four facies associations — topset, foreset, bottomset and offshore marine pelagic deposits. The evidence of Gilbert deltas within open marine deposits reflects the formation of a basin with relatively steep margins connected with a relative sea level fall, erosion and incision. Formation, progradation and aggradation of the thick coarse-grained Gilbert delta piles generally indicate a dramatic increase of sediment supply from the hinterland, followed by both relatively continuous sediment delivery and an increase in accommodation space. Deltaic deposition is terminated by relatively rapid and extended drowning and is explained as a transgressive event. The lower Gilbert delta was significantly larger, more areally extended and reveals a more complicated stratigraphic architecture than the upper one. Its basal surface represents a sequence boundary and occurs around the Karpatian/Badenian stratigraphic limit. Two coeval deltaic branches were recognized in the lower delta with partly different stratigraphic arrangements. This different stratigraphic architecture is mostly explained by variations in the sediment delivery and/or predisposed paleotopography and paleobathymetry of the basin floor. The upper delta was recognized only in a restricted area. Its basal surface represents a sequence boundary probably reflecting a higher order cycle of a relative sea level rise and fall within the Lower Badenian. Evidence of two laterally and stratigraphically separated coarse-grained Gilbert deltas indicates two regional/basin wide transgressive/regressive cycles, but not necessarily of the same order. Provenance analysis reveals similar sources of both deltas. Several partial source areas were identified (Mesozoic carbonates of the Northern Calcareous Alps and the Western Carpathians, crystalline rocks of the eastern margin of the Bohemian Massif, older sedimentary infill of the Carpathian Foredeep and/or the North Alpine Foreland Basin, sedimentary rocks of the Western Carpathian/Alpine Flysch Zone).

Keywords: coarse-grained Gilbert deltas, facies analysis, key stratal surfaces, depositional settings, provenance

Introduction

All major architectonic elements of the foreland basins are conventionally considered to accumulate due to flexural subsidence of the foreland plate, with typical regional orogen-ward thickening on a basinal scale (Beaumont 1981). The classical wedge shape of the basin infill with distinct four depozones, namely wedge-top, foredeep, forebulge, and back-bulge was introduced by DeCelles & Giles (1996). However, modern foreland basins contain a number of smaller-scale depositional features and sedimentary trends, which might be unrecognized in ancient successions owing to the fact that regional data sets are required for their identification (e.g., DeCelles & Cavazza 1999; Shukla et al. 2001; Hartley et al. 2010; Weissmann et al. 2010). When reconstructing fluvial and deltaic stratigraphy it is especially necessary to obtain a regional, three-dimensional data set. Collecting of such a data set is time consuming and complicated. On the other hand, data about the depositional architecture of deltas provide a useful tool in reconstructing the complicated synsedimentary history (interplay between tectonics, eustasy, climate, basin physiography and sediment supply) of the foreland basin. The Neogene Carpathian Foredeep basin provides an opportunity to study the characteristics of a series of marine coarse-grained deltaic systems.

The main aims of the presented paper are: a) to propose a novel interpretation of the Lower Badenian "basal or marginal coarse clastics" in the southernmost part of the Western Carpathian Foredeep as deposits of coarse-grained Gilbert deltas; b) to reconstruct the stratigraphic architecture of these deltas to demonstrate coarse grain delta deposits as an indicator of the infill history of the basin, especially along the basin margins where biostratigraphic evidence is poor; and c) identification of the source area of the deltas.

Geological setting

The Western Carpathian Foredeep Basin represents a peripheral foreland basin formed during the lithospheric flexure of the Bohemian Massif in response to the thrust load of the Western Carpathians and the Eastern Alps. The studied area is part of the southernmost segment of the basin where the Carpathian Foredeep continues into the North Alpine Foreland Basin (Alpine Molasse Zone) in the southwest (see Fig. 1A). The stratigraphic range of the sedimentary infill of the basin

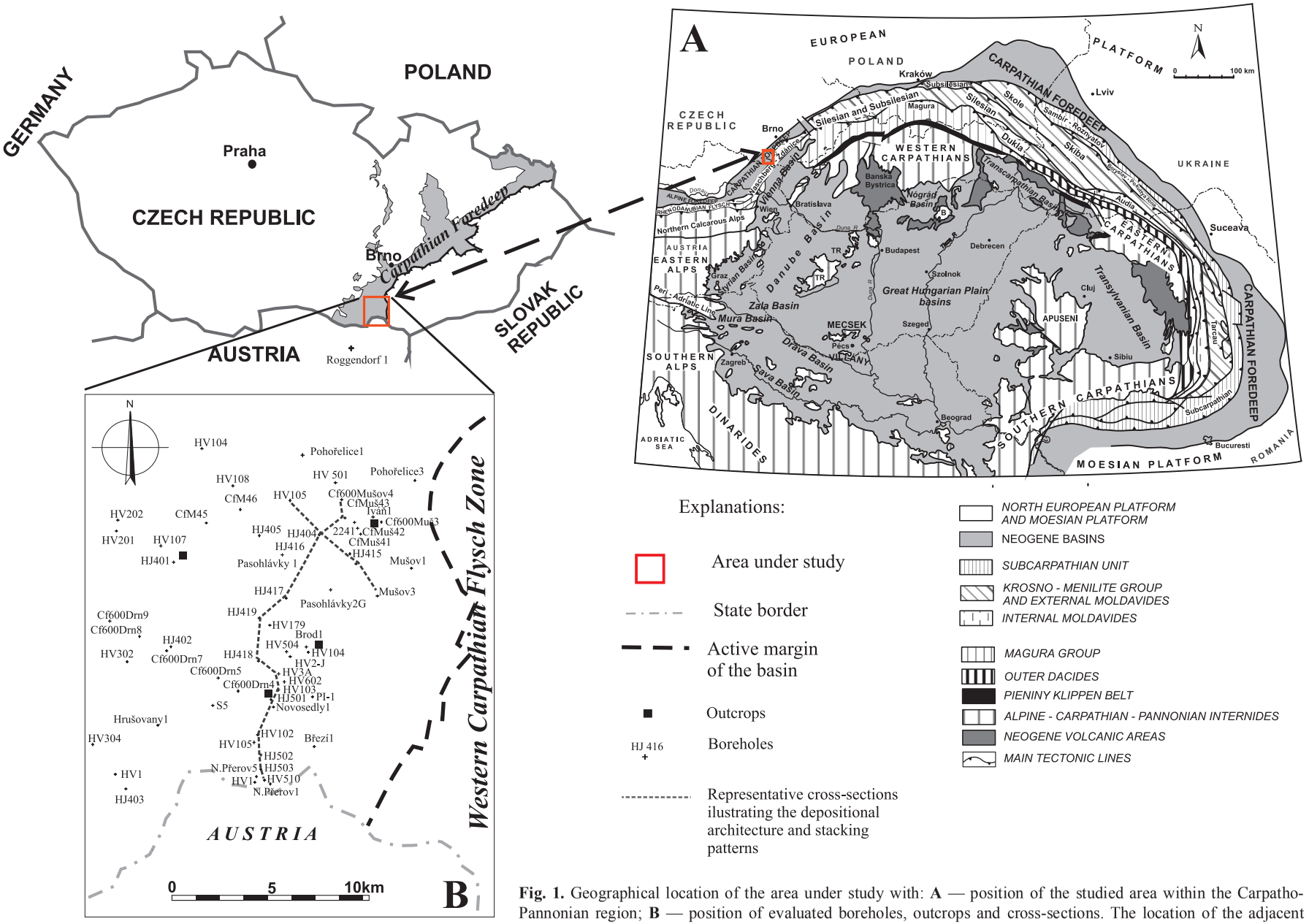

Fig. 1. Geographical location of the area under study with: **A** — position of the studied area within the Carpatho-Pannonian region; **B** — position of evaluated boreholes, outcrops and cross-sections. The location of the adjacent borehole Roggendorf-1 is also indicated.

segment is Oligocene/Lower Miocene (Egerian) to Middle Miocene (Lower Badenian) (Brzobohatý & Cicha 1993). The study area is located above the Iváň canyon, which represents a shelf-indenting canyon that formed due to a combination of isostatic rebound along a terminating thrust front and sea-level change during the terminal Early Miocene/Karpatian (Dellmour & Harzhauser 2012).

The Lower Badenian deposits of the Western Carpathian Foredeep reveal distinctive basin infill geometry because they almost symmetrically thicken towards the basin centre (Nehyba & Šikula 2007). Two lithofacies strongly dominate, both areally and volumetrically. The first lithofacies are monotonous basinal pelites ("tegel") with a maximum thickness of ~600 m in the central part of the basin. The pelites reflect a marine depositional environment of the middle to outer shelf and their abundant fossil content indicates the Middle Miocene (Lower Badenian of Central Paratethys regional stages) age with some evidence for Zone NN5 (Tomanová-Petrová & Švábebnická 2007). A changeable paleoenvironment, especially sea-level fluctuation and unstable conditions were documented (Nehyba et al. 2008). Rare and thin interlayers of acidic tuffs and tuffites are interpreted as distal tephra fallout (Nehyba et al. 1999).

Pelites commonly overlie the other dominant lithofacies, namely "basal or marginal coarse clastics". These sandy gravels and gravelly sands have been evaluated without detailed sedimentological studies by Menčík (1973), Krystek (1974), Novák (1985, 1986a,b) and Stráník et al. (1999) and are known by several local names. They were recognized as a product of Lower Badenian transgression and interpreted as gravel beach deposits (Menčík 1973; Krystek 1974), or shoreline marine bars and marine deltas formed during the end of the Karpatian and start of the Badenian (Stráník et al. 1999). The Lower Badenian age of the gravels was documented by *Uvigerina macrocarinata* and *Orbulina suturalis*, which were recognized in clayey and sandy intercalation in gravels (Čtyroký 1993). These gravels represent an important aquifer of the area (Kryštofová 2007).

Red-algal limestones widely known from the Lower Badenian succession of the basin (Doláková et al. 2008) are very exceptional in the studied area. Thin lignite beds were rarely described within the Lower Badenian deposits in the area under study.

Methods

The study area is located in south-eastern Moravia between the border of the Czech Republic and Austria in the south and the town of Pohořelice in the north. Individual exposures are rare and not extensive here. The paper presented is based on the study of 4 outcrops (Novosedly 48°50'58.2" N, 16°30'47.6" E; Troskotovice 48°54'41.7" N, 16°25'18.4" E; Brod nad Dyjí 48°52'22.3" N, 16°33'24.1" E; Iváň 48°55'47.8" N, 16°34'18.9"E) and the results of 71 boreholes. These boreholes have been drilled during the last six decades and mostly only general descriptions of lithology and stratigraphy are available. Preserved cores are rare, discontinuous and small. The exceptions are represented by two relatively modern boreholes (Iváň 1 and 22-41 D Pasohlávky). Locations of both outcrops and boreholes are shown in Fig. 1B.

Conventional field methods of sedimentological analysis were used, such as detailed logging, measurement of bedding attitude and paleocurrent directions, and a line drawing of bedding architecture on outcrop photomosaics (Tucker 1988; Walker & James 1992; Collinson et al. 2006). Lithofacies analysis in the outcrops is based on primary sedimentary structures and textures. However, facies analysis of borehole cores is based mainly on grain-size, because sedimentary structures were obliterated by drilling in these loose deposits and/or were not recognized in primary descriptons. Lithofacies were grouped into facies associations, meaning assemblages of spatially and genetically related facies, which are also the expressions of different sedimentary environments.

Pebble and cobble petrography, shape and roundness were determined both in outcrops (clasts larger than 1.6 cm) and in borehole cores (data from 8 boreholes — clasts larger than 8 mm). Shape and roundness were estimated mostly visually using the methods of Zingg (1935) and Powers (1953). The maximum pebble/cobble size represents an average of the longest axis (A axis) of the 10 largest found extraclasts in a locality.

Heavy minerals were studied in 18 samples from 4 outcrops and 6 boreholes in the grain size fraction 0.063–0.125 mm. The chemistry of garnet was analysed for 151 grains and the chemistry of rutile is based on data from 31 grains. Electron microprobe analysis was done on a CAMECA SX electron microprobe analyser (Faculty of Science, Masaryk University, Brno). Samples for the chemistry of garnet and rutile originated from the Novosedly and Troskotovice outcrops and the N 1 Novosedly, HJ 401 Troskotovice and IK 1 Iváň boreholes (see Fig. 1).

Ground penetrating radar (GPR) scanning using Pulse Ekko Pro radar, manufactured by the Canadian company Sensor & Software, at a frequency of 50 MHz with an antenna distance of 3 m was employed. The measurement interval was 0.5 m. The field measurement and processing of the data were provided by Kolejkonzult Brno co. A map of the thickness was created in Surfer 7 software (gridding method).

Results

Facies analysis, sedimentology

Sedimentological study of the outcrops led to the distinction of 9 lithofacies and 8 facies have been identified within the borehole cores. Detailed descriptions (lithology, stratification and sedimentary structures) and interpretation of each facies are given in Table 1A,B. The examples of both lithofacies and facies associations within the logged section can be followed in Figs. 2 and 3.

Table 1: **A** — Descriptive summary list of lithofacies of the studied deposits distinguished in the studied outcrops. **B** — Descriptive summary list of lithofacies of the studied deposits distinguished in the studied boreholes.

Table 1A:

Topset (subhorizontal)		
Symbol	**Description**	**Interpretation**
Gm	Clast- to matrix-supported pebble to cobble gravel, massive. Subrounded to well-rounded clasts mostly up to 10 cm in diameter. Matrix formed by coarse grained sand to gravelite. Bed thickness ranges from 25 to 60 cm. Erosive slightly undulated base. Openwork horizons of coarsest clasts (rare cobbles A max. 20 cm) along the base locally with a 'rolling' a(t) b(i) fabric. Rarely flat lying cobbles along the top of the beds. Tabular beds with flat or convex up top.	Sheetflood deposits, bedload deposition of gravel bars — sheet bars (Nemec & Postma 1993)
Gi	Openwork cobble to pebble gravel, Erosive base. Well rounded cobbles up to 25 cm. Rare intraclasts up to 50 cm to the top of the beds. Pebble horizons along the base with 'rolling' a(t) b(i) fabric. Broadly lensoidal beds, bed thickness ranges from 25 to 35 cm, width of the beds over 2m.	Tractional deposition of bedload gravel as pavement and sheet bars (Nemec & Postma 1993; Miall 1996).
Foreset (steeply inclined 20-25º)		
Gms	Massive/structureless gravelite to pebble gravel, pebble to cobble gravel, mostly clast-supported less commonly clast to matrix (very coarse sand–gravelite) supported, non-graded or coarse-tail inversely graded, forming solitary or amalgamated beds 20 to 350 cm thick with non-erosional bases. Cobbles (extraclasts) up to 15 cm, intraclast up to 60 cm. Mostly non preferred orientation of pebbles, rarely elongated pebbles arranged parallel to bedding. Flat slightly irregular non-erosional top and bases, occasional listric shearing bands. Rare shell debris.	Cohesionless debris flows subject to a low to moderate-rate strain (frictional shear regime (Gobo et al. 2015).
Go	Discontinuous horizons or thin lenses of openwork gravel commonly one clast/cobble or boulder thick, or isolated large subspherical clasts. Thickness varies between 15 to 100 cm, clasts commonly oriented parallel to bedding thick, with cobbly downslope 'heads' and upslope-fining pebbly 'tails'. Boulders (intraclasts) up to 350 cm, extraclasts up to 90 cm.	Deposition by debris fall (Nemec 1990), or modified beds by erosional stripping of an overpassing turbidity current (Gobo et al. 2015)
Gs	Alternation of massive clast supported pebble gravel or gravelite beds (2 to 6 cm thick) and thicker (5 to 10 cm thick) beds of very coarse sand to gravelite, faintly laminated. Some beds contain scattered very coarse pebbles at the base. Tabular shape of the beds. Composed beds are up to 250 cm thick.	Deposition of high density turbidity currents (sensu Lowe 1982).
Sl	Mostly fine to medium sand, poorly sorted due to admixture of very coarse sand and rare granules, plane parallel stratification, inclined bedding, bed thickness 4–10 cm, commonly fining upward trend in beds, flat slightly undulated top and bases	Tractional deposition by low density turbidity current (hyperpycnal flow (sensu Lowe 1982).
Smg	Medium to coarse sand, massive, normal distributional grading, sometime passing upward into faintly planar parallel-stratified sand.Bed thickness varies between 10 ad 20 cm.	Deposition by high density turbidity current (sensu Lowe 1982).
Sg	Coarse to very coarse sand, poorly sorted, scattered granules or small pebbles up to 1 cm in diameter, outsized clast are commonly aligned parallel to bedding, massive to faint lamination, alternation slightly finer and coarser grains. Bed thickness varies between 20 ad 40 cm.	Sandy debris flow accompanied or followed by low density turbidity current (Postma et al. 1988; Mulder & Alexander 2001).
Ml	Alternation of laminas or thin beds of very fine sand, planar parallel laminated, micaceous, relatively well sorted, and laminas of dark brown green silt to silty sand, calcareous, faintly laminated to massive.	Traction to suspension deposits of low density turbidity currents

Table 1B:

Symbol	**Description**	**Interpretation**
G1	Massive/structureless pebble gravel, clast to matrix supported, cobbles up to 10 cm. Well rounded pebbles, limestone dominate in the pebble spectra. Both subhorizontal and inclined beds. Horizon thickness highly varies and can reach tens of meters.	Subhorizontal beds — tractional deposition of bedload gravel (Nemec & Postma 1993; Miall, 1996) (Equivalent to Gm, Gi in outcrops). Steeply inclined beds — mass flow deposits, most probably products of cohesionless debris flows, outsized cobbles might be connected with debris fall (Equivalent to Gms, Go in outcrops).
G2	Beds of very coarse sand to gravelite, Some beds contain scattered very coarse pebbles to small cobbles at the base. Large scale cross bedding /foreset sometimes evident. Composed beds are tens of meter thick.	Mass flow deposits, most probably products of cohesionless debris flows, debris fall and turbidity currents. (Equivalent to lithofacies Gs in outcrops)
S1	Fine to medium grained sand, faint to well developed planar paralel stratification. Subhorizontal beds.	Deposition from low density turbidity currents (sensu Lowe 1982). (Equivalent to lithofacies Sl in outcrops).
S2	Medium grained sand, structureless, relatively well sorted. Subhorizontal beds, bed thickness about 20 cm.	Deposition from mass flows - sandy debris flow to high density turbidity currents (sensu Lowe 1982).
S3	Fine to very fine sand, massive scattered pebbles to small cobbles (up to 10 cm in diameter). Sand relatively well sorted. Limestone pebbles dominate in pebble spectra. Subhorizontal beds, thickness of amalgamated beds up to 1.4m.	Deposition from low density turbidity currents (sensu Lowe 1982). Pebbles/cobbles can originate from debris fall.
S4	Rhythmic alternation of laminas of very fine sand and silt, planar parallel laminated or massive silty mud. Typical occurrence of scattered pebbles up to 3 cm diameter, rare cobbles up to 10 cm. Pebble strings or even thin beds (up to 6 cm thick) of gravel (pebbles up to 5 cm in diameter). Pebbles are well rounded, limestone dominates in pebble spectra. Pebble gravels are clast supported to openwork. Subhorizontal beds, individual bed thickness about 20 cm, amalgamated beds several m thick.	Deposition from low density turbidity currents (sensu Lowe 1982), attributed to river-generated hyperpycnal flows descending subaqueous delta slope (Nemec 1995). Scattered pebbles can originate from debris fall. Isolated thin interbeds of facies S4 within monotonous gravel succession can also represent large intraclasts.
S5	Fine to medium grained sand, well sorted, calcareous, massive, shell debris. Subhorizontal beds, bed thickness up to 1 m. Alternation with beds of facies M1.	Occasional input of the sandy material is connected with storms or mass flows into open marine environment.
M1	Grey, green-grey massive silty claystone, calcareous, well sorted, occurrence of shell debris. Subhorizontal beds, bed thickness more than 10 m.	Open marine suspension deposits, hypopycnal suspension plumes? (Nemec 1995)

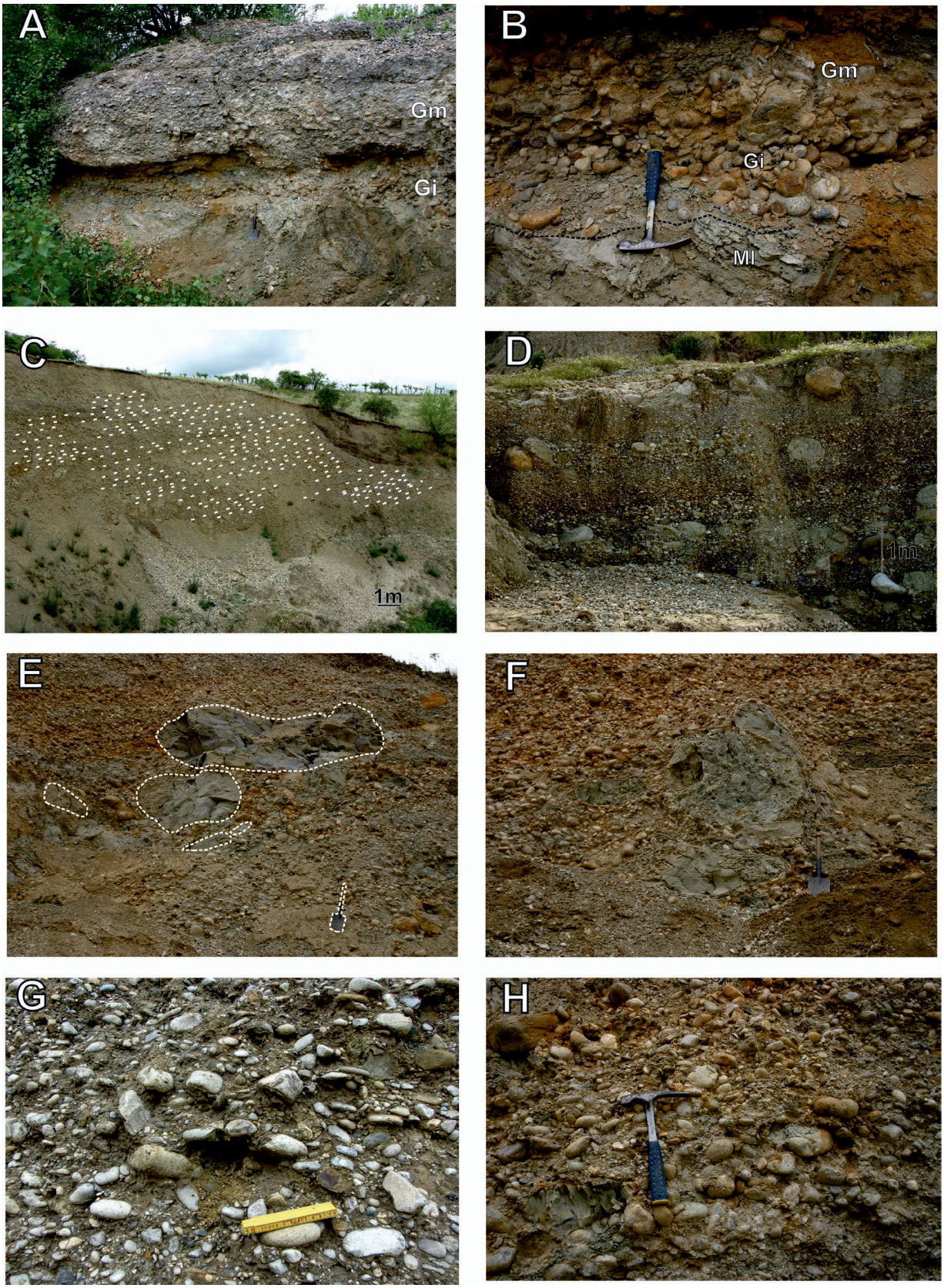

Fig. 2. Selected examples of lithofacies and facies associations: **A** — deposits of FA 1 (topset) — facies Gm and Gi; **B** — contact of FA 1 (topset) and FA 2 (foreset) facies Ml, Gi and Gm; **C** — deposits of FA 2 — large foresets; **D** — deposits of FA 2 (topset) — alternation of facies Gm and Go; **E** — large intraclasts in an early stage of desintegration; **F** — large intraclasts in an advanced stage of disintegration (notice pebble intrusions, coated rims, rounded irregular shape); **G** — facies Gms; **H** — facies Go.

Four facies associations (FA) were identified and for simplicity labelled with interpretive genetic names of depositional environments, but their descriptions are separated from interpretations in the text. They partly (FA1–3) correspond to a complete tripartite (proximal to distal) Gilbert type delta profile. FA1(topset) and FA2 (foreset) were clearly identified in outcrops. However, in many boreholes, commonly "a joint" FA1+2 is declared due to problems with clear identification of FA1 and FA2 (poor primary description). FA3 (bottomset) and FA4 (offshore marine pelagic deposits) were identified only in boreholes. Logs illustrating the distribution of facies associations both from outcrops and boreholes are presented in Figs. 4, 5 and 6.

FA1 — topset deposits

Topset deposits were identified in only one outcrop. Here the facies associations consist of poorly sorted gravels of facies Gm and Gi forming subhorizontal tabular packages about 4 m thick with internal subhorizontal erosional surfaces with relief of several dm (Fig. 2A,B). The presence of fossils was not observed. FA1 deposits are present in some boreholes (facies G1 in the uppermost part of the succession covering facies S1), where they reach a thickness of about 12 m. A fining upward trend is evident. Deposits of FA1 overlie deposits of FA2. Deposits of FA1 or FA1+2 are mostly overlain by deposits of FA4, rarely by deposits of FA3.

Interpretation: Recognized facies are interpreted as bedload deposits (gravel pavement and sheet bars). The sheet-like geometry, limited incision and the lack of cross-stratification suggest deposition of poorly confined flows, in broad and shallow braided channels or overflows during periods of high discharge. Rare evidence of FA1 (compared to FA2) could point to its basinward thinning and/or its formation dominantly during the terminal stage of the delta building. Deposits of FA1 are interpreted as fluvial-dominated topset. Marine influence (wave, tide) was not recognized.

FA2 — foreset deposits

FA2 represents the volumetrically dominant facies association. It consists of steeply inclined (15–25°), tangential, laterally continuous, sandy to gravelly beds oriented at directions of 262°–059°. The logged thickness of FA2 varies between 4 and 21 m; however, its base was not reached (Fig. 2C,D). The thickness of FA2 (or FA1+FA2) in boreholes can reach up to 160 m. Deposits of FA2 here cover deposits of FA3 of FA4 and are covered by FA1 or FA4.

FA2 includes ten lithofacies (i.e. Gms, Go, Gs, Sl, Smg, Sg, G1, G2, S2 and S4); however, only six of them (Gms, Go, Gs, Sl, G1 and G2) form the larger portion of the association (Fig. 3A,B). Common inclined planar parallel stratification is obvious due to minor vertical changes in clast sizes between adjacent strata — commonly only one clast thick — and is highlighted by a plane-parallel clast orientation. Facies G1 and G2 strongly predominate in boreholes, forming 89.5 to 100 % of FA2 there (see Fig. 6). The rest of facies (S2 and S4) form 0 to 10.5 %. Lithofacies Gms and Go (Fig. 2G,H and Fig. 3A, B) mostly predominate on outcrops, forming 38.9 to 100 % of FA2 there (see Figs. 4 and 5). Lithofacies Gs and Sl (Fig. 3C and D) form a significant portion of FA2 in one outcrop and represent 34 to 57 % of the facies succession there (see Fig. 4B,C). Cobbles and boulders of mudstone intraclasts were recognized in various stages of disintegration (angular boulders with well preserved internal stratification vs. highly irregular, rounded cobbles with irregular intrusions of pebbles; sharp margin of clasts vs. coated rim of small pebbles) (Fig. 2E,F).

Interpretation: Lithofacies Gms represents cohesionless debris flows, lithofacies Go is interpreted as debris fall deposits. Lithofacies Gs and Sl are deposits of high- and low density turbidity currents. Facies G1 and G2 are interpreted as gravity flow deposits — products of cohesionless debris flows, debris fall and high density turbidity currents. Facies S2 and S4 are products of sandy debris flows or low and high density turbidity currents. The lithofacies assemblage suggests steep delta foresets dominated by the deposition of gravity flows (Nemec 1990b). Evidence of a large scale foreset clearly points to a Gilbert type delta. Gilbert deltas (Gilbert 1885) are defined by their tripartite geometry of sub-horizontal topsets, steeply inclined foresets and sub-horizontal bottomsets. Gilbert-type deltas form in settings where the depth ratio (channel depth over basin depth) is small and where bedload transport is high. Variations in the direction of the dip of foreset are explained by evidence of several shifting deltaic lobes. Superposition of shifting lobes was evident also from the facies architecture of the outcrop. The progradation generally towards WNW-NE points to the position of the deeper parts of the basin.

The situation on the outcrops points to either debrite-dominated foreset deposits (more common) and/or turbidite-dominated foreset deposits (less common) (Gobo et al. 2015). The different delta-slope sedimentation processes in these cases might reflect the delta-front morphodynamic responses to base-level changes, namely either (relatively more common in the studied case) increased accommodation (relative sea level rise) or deficit of the delta-front accommodation (stillstand or relative sea level fall) (Gobo et al. 2015).

The described Gilbert-type delta deposits consist mainly of sandy gravels and gravelly sand. Paucity of mud in the matrix and the common occurrence of mud intraclasts is typical. The separation of the muddy fraction from the coarse (sand+gravel) fraction is explained by the density contrast between the sea water and the inflowing river water. Whereas low-density fresh water plumes carried suspended sediment out to sea, bedload sediment was damped close to the river mouth. Mud-poor gravel mixtures avalanched for relatively short distances; the lack of mud results in strong frictional forces between the clasts. This lowers the mobility of the sediments and thus increases the stability of the slope and allows the development of steep coarse-grained foresets (Nemec 1990 b).

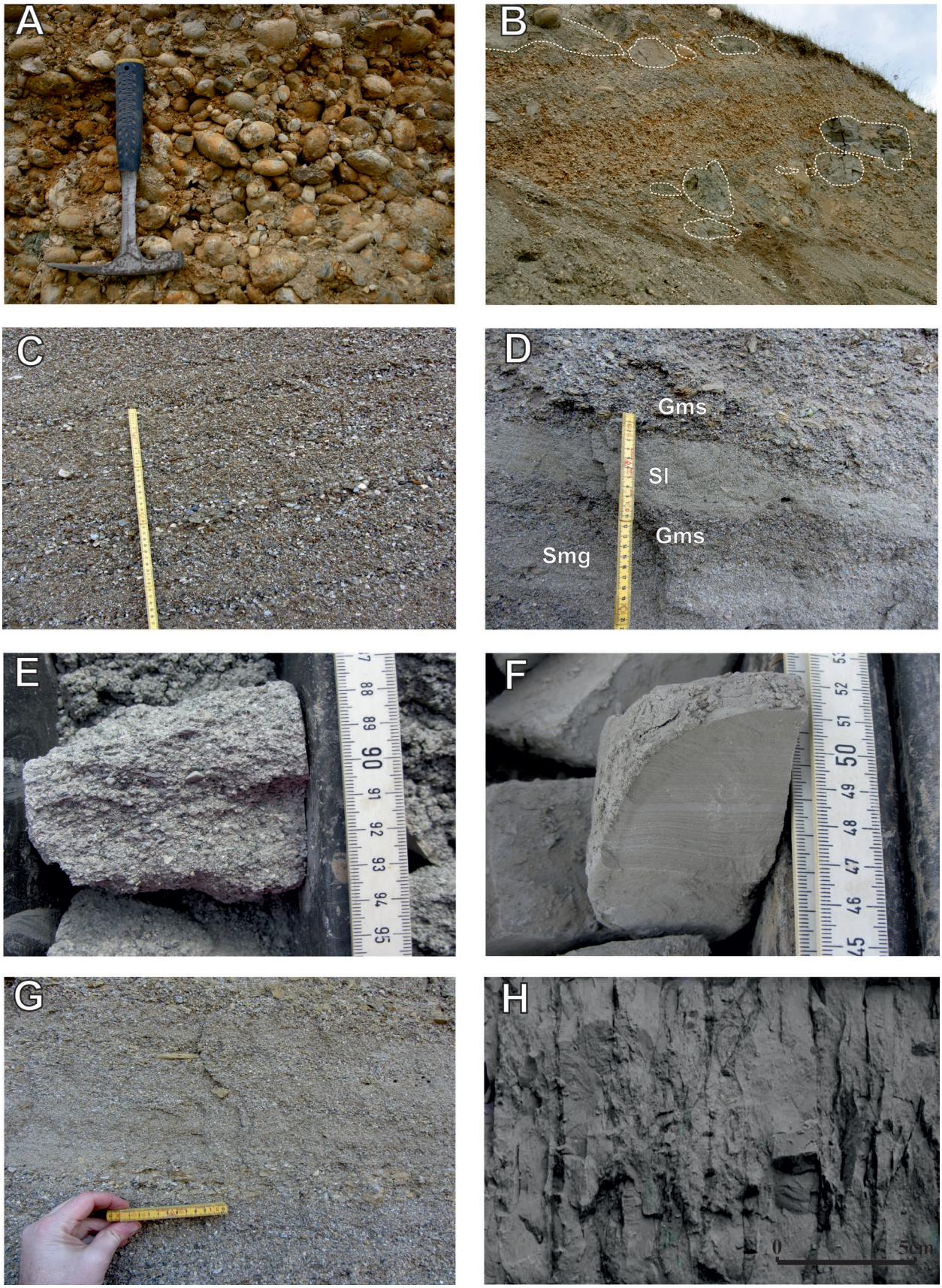

Fig. 3. Selected examples of lithofacies and facies associations: **A** — facies Go; **B** — alternation of facies Gms and Go; **C** — facies Gs; **D** — alternation of facies Gms and Sl; **E** — facies G2; **F** — facies Ss; **G** — facies Smg; **H** — facies M1.

The presence of floating intraclast indicates that the gravity flows were erosive at some stage. These intraclasts were mostly eroded from exposed older Neogene basin infill or from a delta plain. The semi-consolidated mud clasts will normally become subject of disintegration during transport. However, if an initial damping of turbulence occurs at the same stage as erosion (rapid transformation of the flow behaviour), the suspended intraclasts may survive intact (Postma et al. 1988). The mud clasts largely moved over rather short distances (a few hundred metres) and came to rest upon the steep foresets. The outsized clasts are randomly scattered within the succession of FA2, occasionally forming clusters. Occurrence of outsized boulders suggests a steep slope over which sediments can gain high downslope mobility overcoming the frictional resistance of the substratum.

The steeply inclined bedding, parallel to the depositional slope, and large height of the preserved delta slope deposits suggest that the coarse-grained Gilbert delta was formed along a steep margin. The 150 m thickness of FA2 points to a relatively deep basin (a reasonable minimum estimation of the paleowater depth is the second tens of m) and intense sediment supply. With sufficient bedload material transported to the delta rim, the delta slope may have prograded as a result of semicontinuous to continuous downslope movement of sediment (Nemec 1990b; Eilertsen et al. 2011). Heavily laden traction currents at the river mouth may have continued downslope as gravity-driven underflows during major floods (Massari & Parea 1990).

FA 3 — bottomset and prodelta deposits

The thickness of this facies association varies between 0 and 58 m. FA3 shows flat laying beds and comprises five lithofacies (lithofacies G1, S1, S2, S3 and S4). Whereas occurrence of lithofacies G1 and S1 is rare (they are commonly missing, rarely reach up to 8 %) and they form relative thin interbeds, lithofacies S4 is the most common (Fig. 3F). Two lithofacies assembleges were identified: i) monotonous monofacies assemblages (mostly lithofacies S4, rarely S2); ii) interbedded lithofacies assembleges (lithofacies G1, S1, S2, S3 and S4; but with a strong prevalence of lithofacies S3 and S4) with generally coarsening upward trends. Both the top and base of FA3 are sharp and abrupt. Deposits of FA3 mostly overlie deposits of FA4, less commonly deposits of FA1–2. Deposits of FA3 are mostly overlain by deposits of FA1–2, less commonly by deposits of FA4.

Interpretation: The dominant lithofacies S4 and also lithofacies S1, S2, and S3 are interpreted as deposits of high- or low density turbidity currents. Unique occurrence facies G1 is interpreted as an arrival of mass flow deposits (cohesionless debris flow) on the shallowly dipping delta front or deposits of hyperpycnal flows (Mutti et al. 2003). These observations correspond to the deposition of a subaqueous delta base where foresets pass into more gently dipping horizontal bottomsets (Backert et al. 2010). The coarsening upward trend is explained by transition from distal to proximal bottomset.

Bottomsets were defined by Gilbert (1885) as gently inclined ($\leq 10^{o}$) fine grained sediments. Similarly Colella (1988) or Nemec (1990a) point to their "low angle" dip and Massari & Parea (1990) or Chough & Hwang (1997) point to their 'fine-grained' nature. Bottomsets are here defined similarly as by Ford et al. (2007) or Backert et al. (2010) as the down-dip terminations of foresets, where the facies association is transitional, deposited by both gravitational flow and suspension fallout processes. The facies transition can be abrupt or very gradual. Variations in thickness of the bottomset deposits probably reflect a lobate shape, common at the base of steep-gradient delta slopes (Lee & Chough 1999). The pebble- to cobble-sized openwork gravel lenses in thin to medium-thick sandstone beds are typical of mass-flow-dominated deposits at the base of gravelly steep-gradient delta slopes and prodelta environments (Postma & Cruickshunk 1988; Lee & Chough 1999). The scattered pebbles and cobbles were emplaced by coeval debris falls from the steep foreset slope (Nemec et al. 1999) or, alternatively, may represent outrunning clasts from cohensionless debris flows (Sohn et al. 1997).

FA 4 — offshore marine deposits

The facies association comprises tens to hundreds of metre-thick successions, in which mudstones (facies M1) absolutely predominate (Fig. 3H). The mudstones are generally massive to faintly laminated and contain thin sandstone interbeds (facies S5) or randomly scattered sandy grains. Mudstones are calcareous and rich in marine fossil content. FA4 occurs either above or below FA1, FA2 and FA3. FA4 was rarely recognized interfingering within deposits of FA3 and FA2.

Interpretation: Deposits of FA4 are interpreted as suspension fallout deposits in an offshore marine pelagic environment. The transport of the mud into the basin might be (partly?) connected with river-derived hypopycnal suspension plumes (Nemec 1995). Contact of the basinal clays (FA4) and gravels (FA1+2) is attested as the topset breakpoint path (Backert et al 2010). Such a topset breakpoint path is a key stratal surface, which records a significant landward facies shift and indicates a rapid increase in accommodation/sediment supply. Deposits of FA4 occur below and above the deposits of coarse grained deltas, so they are either Karpatian or Lower Badenian in age (Čtyroký 1993; Stráník et al. 1999; Tomanová-Petrová & Švábenická 2007; Nehyba et al. 2008).

Areal distribution and stratigraphic architecture

Investigations into the stratigraphic architecture are based mainly on borehole data. The total thickness of the "basal or marginal coarse clastics" (namely the Gilbert delta deposits) ranges from zero to 158.5 m (Fig. 7) in the area under study and the greatest one was found around borehole HJ417. Menčík (1973) estimated their maximum thickness at about 190 m. Coarse clastics are generally prolonged in the SW–NE direction along the active margin of the basin with a general

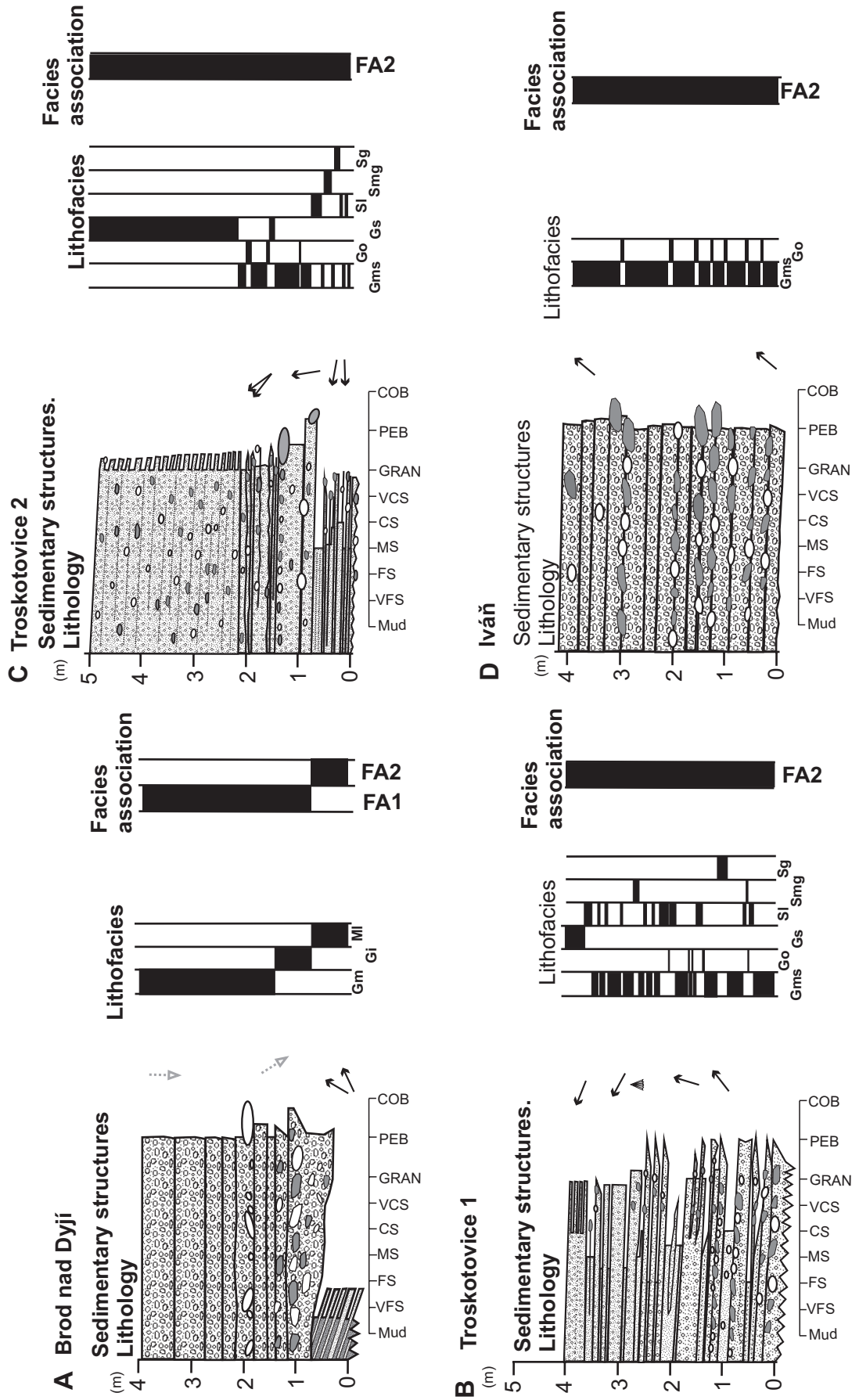

Fig. 4. Sedimentological core logs of outcrops: **A** — Brod nad Dyjí; **B** — Troskotovice 1; **C** — Troskotovice 2; **D** — Iváň.

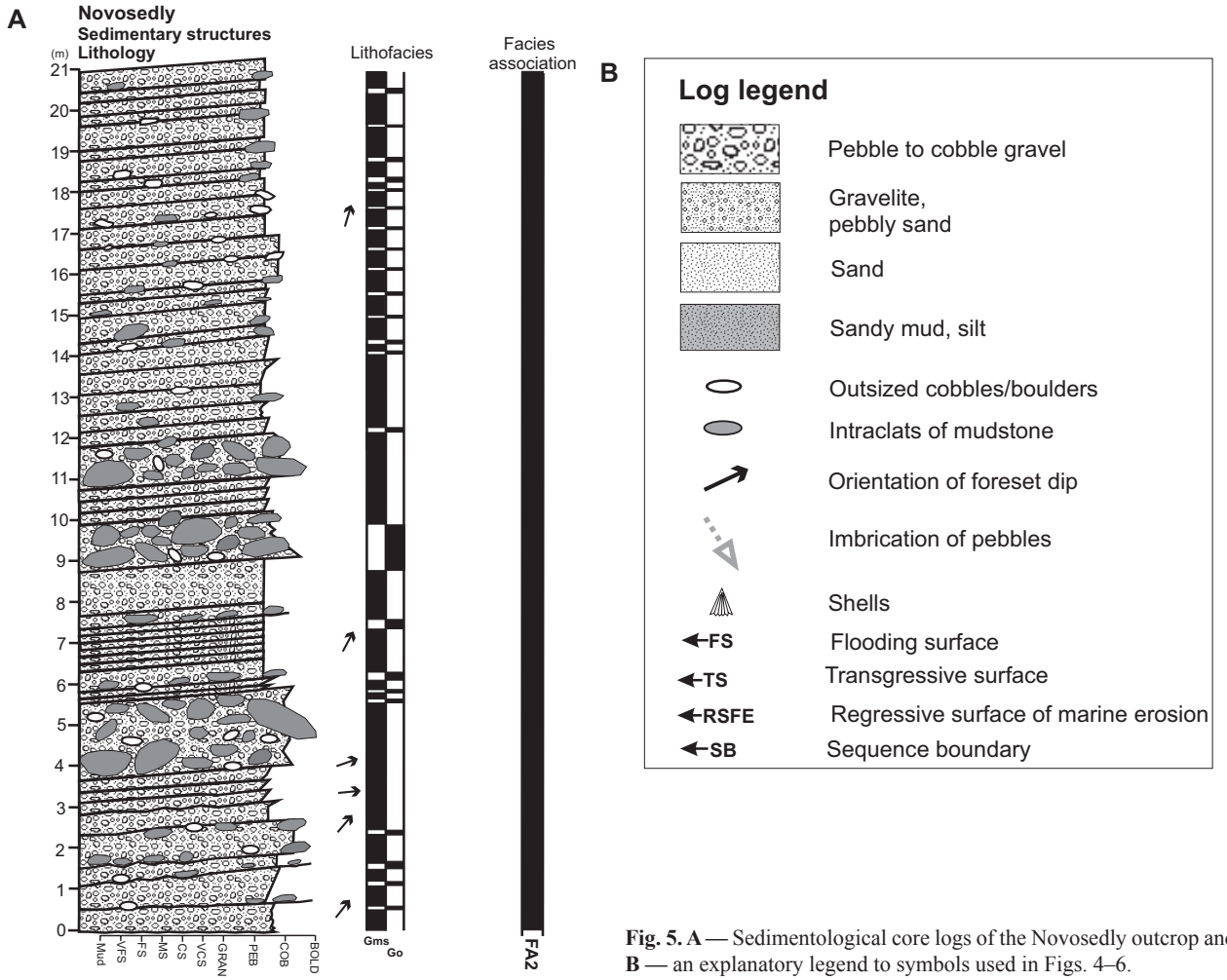

Fig. 5. A — Sedimentological core logs of the Novosedly outcrop and **B —** an explanatory legend to symbols used in Figs. 4–6.

trend of basinward (westward) thickening. The area of the maximum total thickness of clastics generally coincides with the area of the maximum thickness of total succession of the Lower Badenian deposits (Nehyba & Šikula 2007). A significant role of post Badenian tectonics was not documented from the area under study.

Delta architecture is simplified and projected onto two profiles, one NW to SE (Fig. 8A) and the other NNE to SSW (Fig. 8B). The borehole data shows that two deltas can be identified in the area under study with different areal extent, thickness and stratigraphic position. Several key stratal surfaces (KSS) separating individual FA packages are identified and correlated across significant parts of the deltas.

The lower delta (D1) represents the main deltaic body with significantly higher thickness and areal extent than the upper delta (D2). The lower boundary/base of D1 deposits, namely KSS 1 corresponds to the laterally traceable surface, separating the underlying basinal mudstones of FA4 and overlaying coarse grained deposits of FA1+2 or FA3. The D1 occurs in two segments/deltaic branches. The thickest deposits represent the axial portion of the delta branch. Lateral (interbranche) and distal areas are represented by thinner deposits. The two deltaic branches are partly spaced in a basinward position and they are in contact with each other in a landward position. The northern branch is prolonged by about 6 km in a SE–NW direction and by about 7 km in a NE–SW direction, so it covers a surface area of about 28 km^2. The southern branch is prolonged by about 9 km in a SE–NW direction and of about 5.5 km in a NE–SW direction, so it covers a surface area of about 30 km^2. The spatial position of the two branches resembles two divergent aprons (see Fig. 7). The partly different stratigraphic arrangement and different occurrence of KSS can be followed in these two deltaic branches. The northern delta branch is characterized by the spread of FA1+2 deposits over a wide area, relatively uniform lithology, evidence of only two KSS (KSS 1 on the base and KSS 7 on the top) and significant thickness (up to 110 m). However, variations in the tilt of both KSS 1 and KSS 7, together with variations of thickness of FA1+2 in individual cores in the basinward direction and the vertical and lateral arrangement of the deposits (see Fig. 8A), all point to more complex pattern of the northern branch of D1. The southern branch is characterized by multiple alternation of FA1+2 and FA3 deposits, their interfingering with FA 4 (especially in the southern margins of the delta), relatively common and thick FA3 deposits spread over a relatively wide area and significant total thickness of deltaic deposits (up

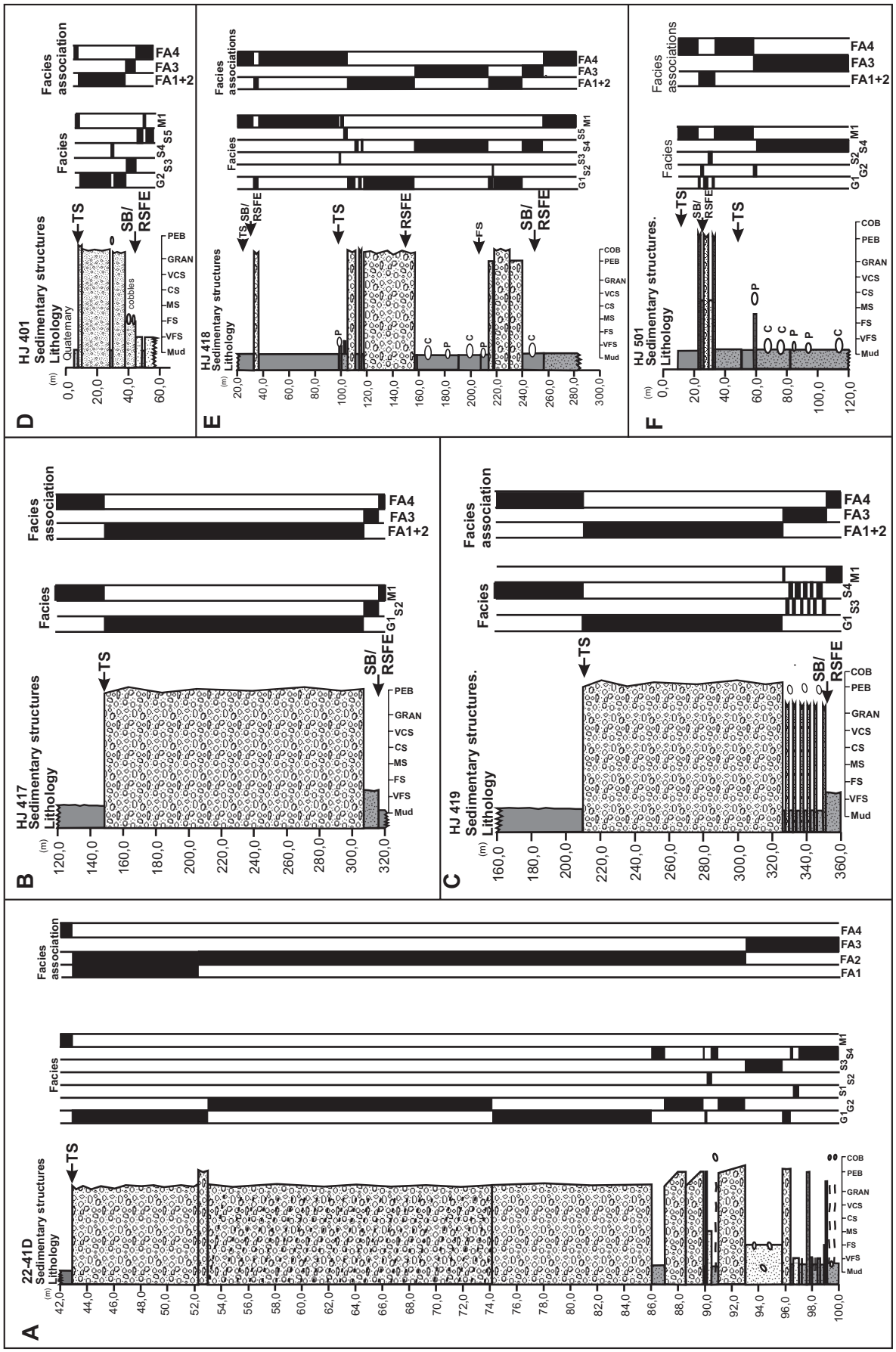

Fig. 6. Sedimentological core logs of the selected boreholes: **A** — 22-41D Pasohlávky; **B** — HJ 417; **C** — HJ 419; **D** — HJ 401; **E** — HJ 418; **F** — HJ 501. The logs show the stratigraphic distribution of sedimentary facies (letter codes as in Table 1) and distinction of facies associations (FA 1–4).

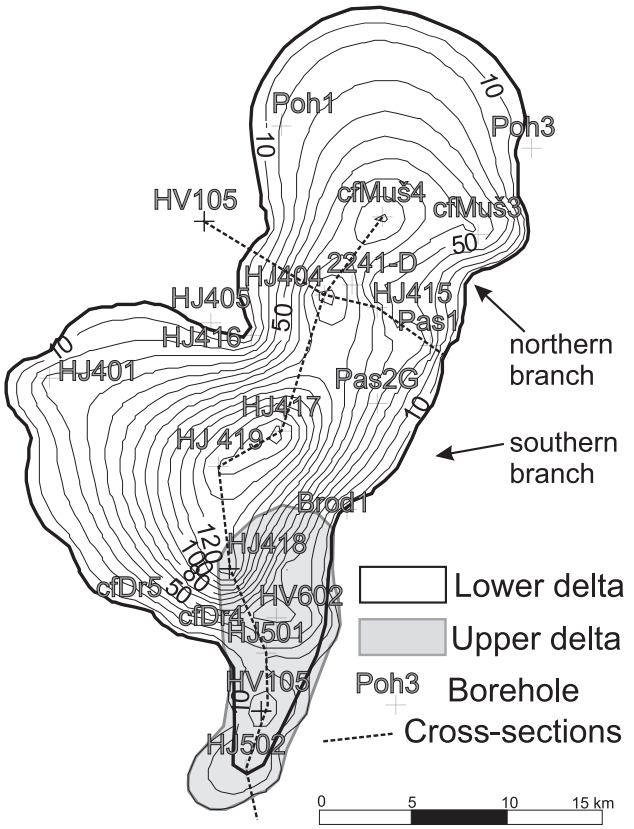

Fig. 7. Areal extent and map of thickness of deposits of both Lower and Upper Gilbert delta (northern branch of lower delta D1, southern branch of lower delta D1).

to 150 m). Such an arrangement points to alternation of delta progradation, retrogradation and aggradation. Several stratal surfaces are identified in the southern part of the southern branch. KSS 2 separates underlying FA 3 deposits and overlying FA 1+2, reflecting a D1 progradation stacking pattern (followed by aggradation). KSS 3 separating FA 1+2 and overlying (onlapping) FA 4 continues towards the N into KSS 4 separating FA 1+2 and overlying FA 3. Both surfaces reflect a retrograding stacking pattern. KSS 5 separating FA 4 and overlying FA 3 reflects a renewed progradation of the delta branch. Further progradation is also reflected by successive KSS 6 separating FA 3 and overlying FA 1+2. All KSS 2–6 are not laterally continuous through D1, but disappear towards the north within a uniform FA 1+2 package. The final KSS 7 represents the top of the D1 and separates underlying FA 1+2 or FA 3 deposits and overlying FA 4. KSS 7 records a significant retrogradation/landward shift in the topset breakpoint path and finally termination of the deposition of D1.

Upper delta D2 was recognized only in the southernmost part of the area under study (see Fig. 7). D2 is significantly smaller in both thickness and areal extent than the lower delta D1. The maximum total thickness of D2 reaches 33 m. D2 is markedly prolonged in the NE–SW direction, where its radius reaches about 5 km. However, prolongation in the SE–NW direction is only 1.5 km. D2 covers a surface area of about 7 km^2. Lateral and vertical/stratigraphical separation of D1 and D2 suggests migration of the delta depocentre and evolution of the basin margin. Several stratal surfaces are identifed in D2. KSS 8 separates underlying pelagic mudstones of FA 4 from overlying FA 1+2 or FA 3 reflects relative sea level fall followed by progradation and aggradation of D2. KSS 9 separating underlaying FA 3 deposits and overlying FA 1+2 reflects D2 progradation (followed by aggradation). KSS10 represents the top of D2 and separates underlying FA 1+2 and overlying FA 4. KSS 10 records a significant retrogradation/landward shift in the topset breakpoint path and finally termination of the deposition of D2.

Interpretation: The stratigraphic arrangement of Gilbert deltas is directed by the interplay between the available accommodation space/A and the sediment supply/S, expressed as the "A/S ratio" (Jervey 1988; Muto & Steel 1992, 1997; Dart et al. 1994; Martinsen et al., 1999; López-Blanco et al. 2000; Backert et al. 2010; Martini et al. 2017). Accommodation can be created by several factors, most notably tectonic-driven subsidence and rises in base level and sea level (Gawthorpe & Collela 1990; Blum & Tornqvist 2000). When $0<A/S<1$ progradational stacking patterns are developed, when $A/S>1$ retrogradational stacking patterns are developed and when $A/S=1$, aggradational patterns are observed (Shanley & McCabe 1994). Each recognized KSS represents a change in A/S ratio (Backert et al. 2010).

The basal surface KSS 1 of D1 reflects incision, significant migration of the basin depocentre and the start of development of the Gilbert-delta, which is interpreted as reflecting a new basin physiography with relatively steep margins connected with a relative sea level fall (Sohn et al. 2001). The evident convex down shape of KSS 1 (see Fig. 8A) points to a major erosion surface incising downward several tens of m into the Karpatian Laa Fm. and also several km basinward. KSS 1 is regarded as a sequence boundary (similarly Nehyba & Šikula 2007). Progradation (followed by aggradation) of the FA 3 deposits and significant km-long progradation of stacked packages of FA 1+2 gravels observed above KSS1 indicate a dramatic increase of sediment supply from the hinterland. Arrangement of the northern branch of D1 reveals a strong progradation and aggradation stacking pattern of the depositional system, a relatively "continuous" sediment supply and "continuous" low available accommodation space over the time available. Spread of the thick monotonous coarse grained FA 1+2 deposits might suggest a general progradation and aggradation motif for the northern branch — namely $A/S>1$ or $A/S=1$. However, the northern branch of the D1 succession is composed of multiple stacked retrograding deltaic clinoforms (instead of one thick delta pile). Although the generally retrograding stacking patterns are evident from the Fig. 8A, the clear identification of individual stages of D1 evolution or identification of individual deltaic clinoforms is not possible.

On the other hand, the succession in the southern branch of D1 reveals a more complicated arrangement with alternation of phases of progradation ($A/S>1$) and retrogradation ($A/S<1$). KSS 2 suggests a relative increase in A/S ratio, continuing

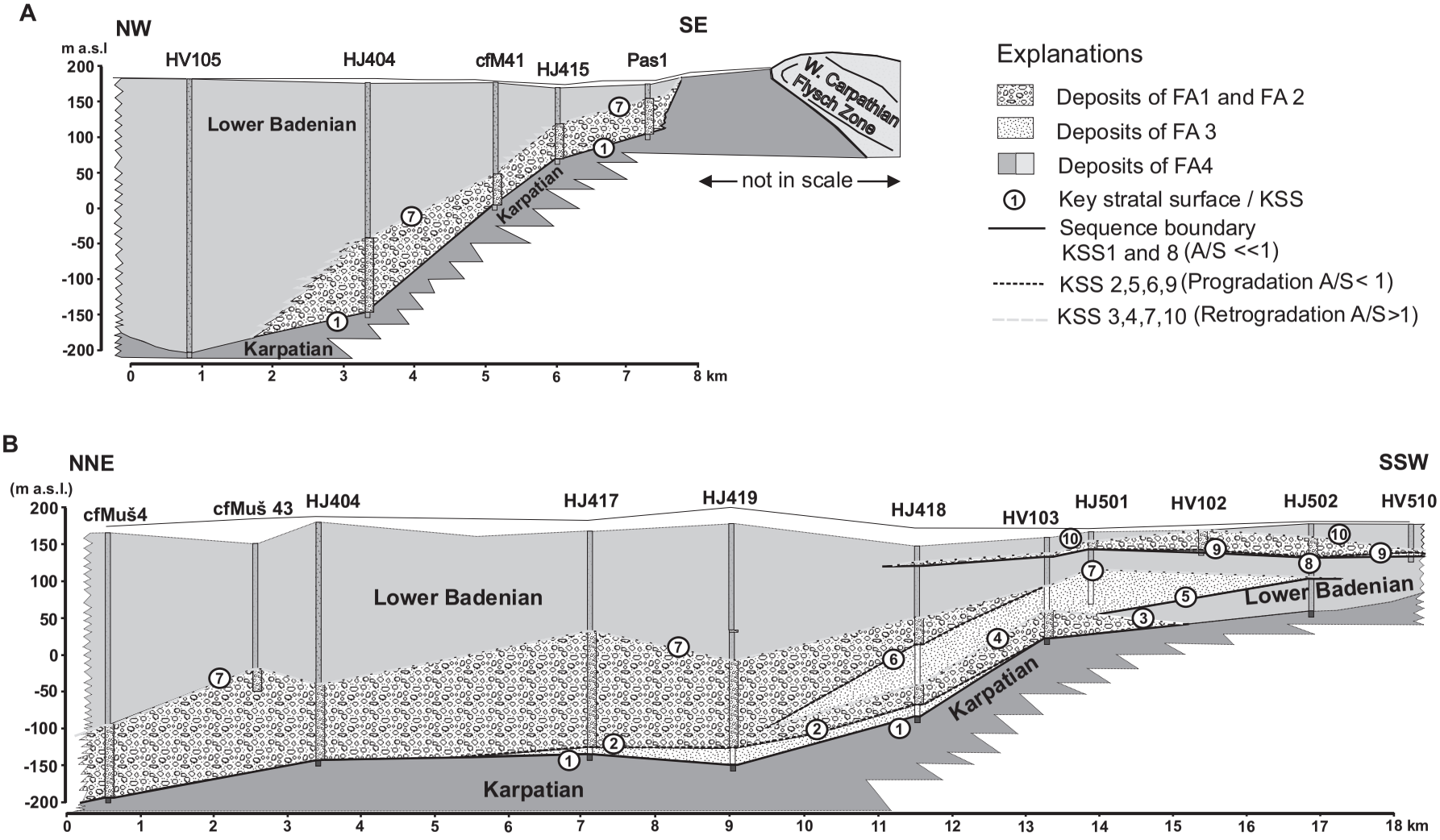

Fig. 8. Representative cross-sections across the studied part of basin with occurrence of Gilbert deltas with position of key stratal surfaces: **A** — cross-section oriented in NW–SE direction; **B** — cross-section oriented in NNE–SSW direction.

progradation and aggradation of D2 after the start of its deposition. Local evidence of KSS 2 points to a cuspate shape of the surfaces cut down into FA 3 beds by overlying large foreset packages (FA 1+2) and may be related to local erosional processes at the foot of prograding foresets.

The thick pile of FA 1+2 above KSS 2 reveals a continuing progradation and aggradation stacking pattern (A/S close to 1). Especially KSS 3 and KSS 4 are obvious expressions of an increase in A/S ratio and retrograding stacking pattern. KSS 5 and KSS 6 points to a decrease in A/S ratio and renewed progradation of the delta branch. The KSS 3, 4, 5 and 6 reveal the same stacking pattern in different (i.e. proximal vs. distal) settings. The deposition of both northern and southern branches is terminated by KSS 7 and connected with the drowning of the D1 delta plain/topset. KSS 7 therefore reveals a significant rapid increase in A/S ratio, rapid retrograding stacking pattern, landward shift of the topset breakpoint and termination of D1 deposition and therefore is connected with a transgressive event.

The stratigraphic evidence suggests coeval deposition of both the delta branches, so the climatic and eustatic sea level factors influenced the whole of D1 in the same way. Although the total thickness of coarse-grained delta deposits is generally comparable in both branches, a greater thickness was recognized in the southern branch. Similar evidence of progradation above the basal surface KSS 1 reflects that erosional period which occurred during a relative sea-level fall was followed by an increase in A/S ratio. Such a situation indicates that the accommodation space was initially formed almost uniformly in the whole area under study. Thus, the differences in the stratigraphic architecture of the northern and southern branch of D 1 might be connected with variations in sediment delivery (Martini et al. 2017) or might result from predisposed paleotopography (by incision) and paleobathymetry of the basin floor. Lateral shifts of position of D2 compared to D1 generally towards the SSE, both the more complex stratigraphic architecture and the higher thickness of southern branch of D1 towards the southern margin of D1 might reflect varied position of the deltaic entry to the basin and/or indicate a relatively rapid formation of accommodation space towards the southern part of the basin during the studied stratigraphic interval. This situation might be connected with the position of the drainage system, or with possible connection between the Vienna Basin and the Carpathian Foredeep (Brzobohatý & Stráník 2011).

The evolution of D2 is less complicated as it predominantly records progradation. KSS 8 as the base of D2 reflects a significant decrease in A/S ratio (interpreted as a relative sea level fall) and "localized" formation of a steep basin margin. The progress of progradation and aggradation of coarse-grained Gilbert delta deposits is connected with increase of accommodation space. KSS 9 suggests a relative increase A/S ratio, continuing progradation and aggradation of D2. Local evidence of KSS 9 points to a cuspate shape of the surfaces cut down into FA 3 beds by overlying large foreset packages. It is proposed that KSS 2, 6 and 9 record local erosion due to emplacement processes at the base of prograding foresets (FA 1+2). These surfaces are therefore autocyclic erosional surfaces that post-date the increase in A/S (Backert et al. 2010). The thick pile of FA 1+2 above KSS 9 reveals a continuing progradation and aggradation stacking pattern, so an A/S ratio close to 1. KSS 10 representing the top of D2 records a significant retrogradation stacking pattern, flooding, landward shift in the topset breakpoint and finally termination of the deposition of D2, all indicating a rapid further increase in A/S ratio due to transgression. The KKS 10 is relatively flat, pointing to a flat delta plain and rapid flooding. Debrite-dominated foreset deposits are typical for the upper delta D2.

A marked bathymetric gradient towards the west or north-west and south-west in the area under study indicate that the basin axis was probably influenced by the active (eastern) basin margin. Although the position of studied coarse grained deltas generally coincides with eastern wall of the Karpatian Iváň canyon (Dellmour & Harzhauser 2012), the studied deltas are not parts of the canyon infill. The top part of the canyon was eroded around the Early/Middle Miocene boundary, capped by marine marls during the subsequent early Middle Miocene transgression, and also the seismic data does not show the presence of deltaic foresets (see Dellmour & Harzhauser 2012). However, presence of this structure might have affected the predominant Neogene drainage system of the area (differential subsidence and more rapid formation of the accommodation space) and the actual position of the deltas. The marked prolongation of D2 in the N–S/SW direction together with the orientation of the foreset dip on outcrops (NNE-NE ward) point to the existence of several delta lobes and complex progradation generally basinwards.

Ground penetrating radar

Two georadar cross sections were measured in the locality of Novosedly. The longer cross section L0 shows the internal organization of the studied deposits of upper delta D2 in the NW–SE direction and the shorter cross section L1 reflects the internal organization of D2 in the NNE–SSW direction (Fig. 9A, B, D). Georadar profiles were oriented along the outcropped walls of the sand pit, so the image can be to some extent calibrated by the visually observed depositional settings. Four main georadar units (GRU) were defined based on the characteristic reflection configuration (parallel to sub-parallel reflections in each unit) (Fig. 9C, E).

GRU 1 is characterized by continuous, horizontal, planar to slightly undulated parallel reflections and was developed in the uppermost part of the profile. GRU 1 is of tabular shape, its thickness is relatively stable between 1 and 1.5 m and its base is almost flat. GRU 2 is characterized by low amplitude, highly variable (slightly undulated to almost planar, short, horizontal to subhorizontal, sub-parallel) reflection. GRU 2 is of slightly irregular shape with both base and top undulated; however, the base is significantly more uneven than the top. The thickness of the unit varies between 0.5 and 1.5m (due to the uneven base), but is mostly about 1 m. The base of the unit truncates

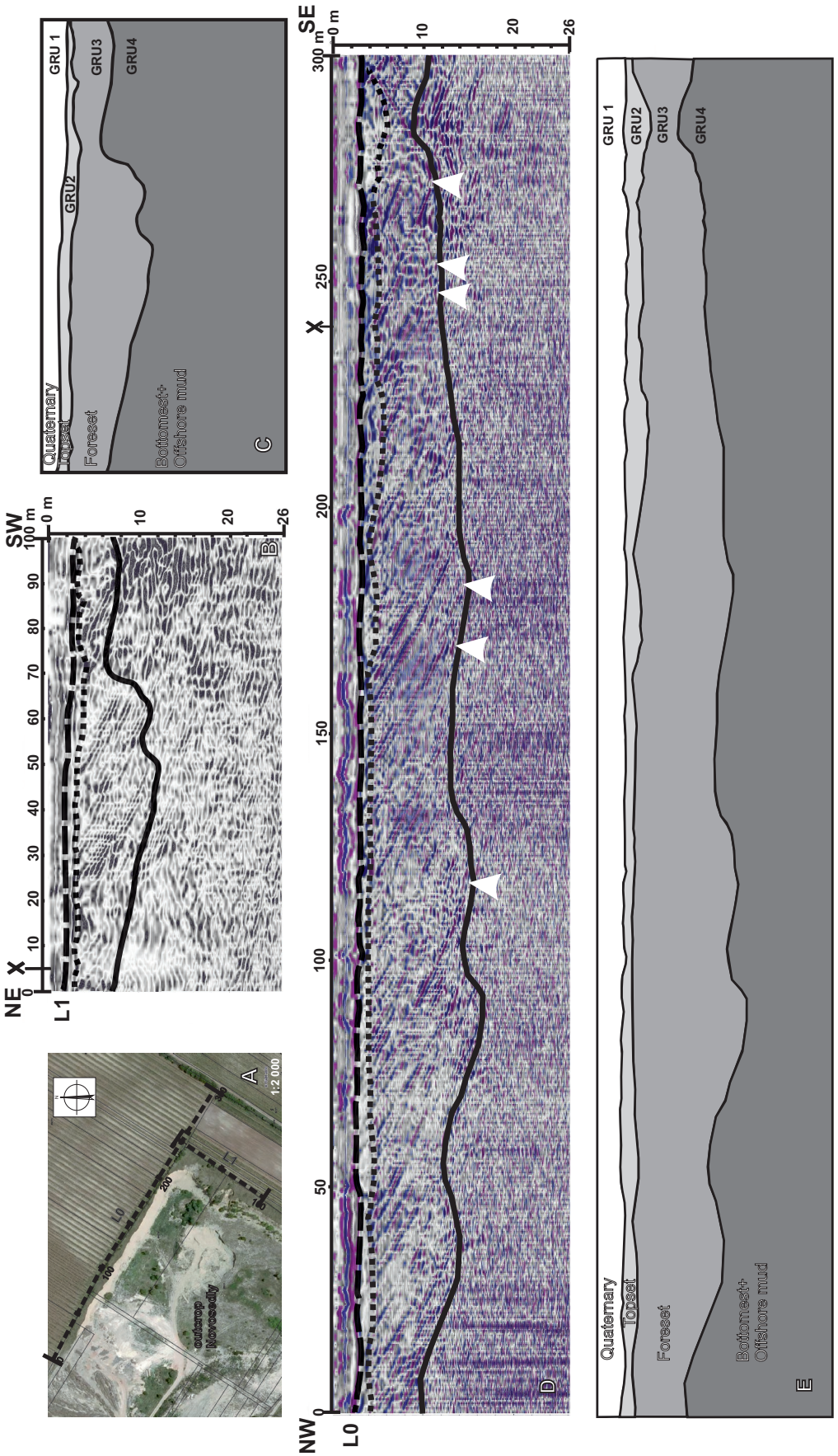

Fig. 9. Ground penetrating radar profiles across the Novosedly outcrop. **A** — Location of profiles; **B** — Profile L1 - raw data; **C** — Profile L1 - interpretation; **D** — Profile L0 - raw data; **E** — Profile L0 - interpretation. White arrows mark scoop-shaped scours.

the underlying reflections of GRU 3. GRU 3 is generally characterized by the dominance of steeply inclined reflections. These reflections are generally continuous and parallel. Occasionally, short, horizontal, concave up and concave down reflections occur between more continuous dipping reflections. The top of GRU 3 is slightly irregular (undulated). The base of GRU 3 is very uneven, with numerous significant undulations (see white arrows in Fig. 9D). The thickness of GRU 3 ranges from 6 to 12 m and the unit is of generally tabular to wedge shaped. GRU 4 is generally characterized by mostly discontinuous, short, horizontal, planar to concave up or concave down reflections. GRU 4 forms the lower parts of the profile. The contact between GRU 3 and GRU 4 is mostly sharp and very uneven. Transition from GRU 3 into GRU 4 was observed only rarely and is connected with the gradual passage of inclined reflections to flat laying horizontal ones (gradual decrease of the dip).

Interpretation: The comparison of the GPR profiles with depositional setting in the outcrop walls shows that GRU 1 represents the Quaternary sedimentary cover. GRU 2 is interpreted as deposits of FA 1. Continuous, horizontal to subparallel, and in places hummocky reflections sharply truncating underlying inclined reflections of foreset are typical of fluvial topsets of Gilbert deltas in GPR cross sections (Jol & Smith 1991), and are generally also characteristic for alluvial horizontally bedded sands and gravels (Ékes & Friele 2003). GRU 3 is compared with FA 2. This interpretation is confirmed by inclined continuous (large scale) parallel reflections with some differences in the dip, which are typical of the GPR record of the foreset (Roberts et al. 2003; Eilertsen et al. 2011). The upper boundary of GRU 3 with overlying GRU 2 is interpreted as toplap, and contact with underlying GRU 4 as downlap. Toplap of inclined reflections (GRU 3) in contact with subhorizontal reflections (GRU 2) reveals the erosional relation of the topset and foreset. Variations in continuity, frequency and also in the orientation of the dip of individual series of inclined reflections reveal variations in the type of mass flows (turbidity currents vs. debris flows). Short subhorizontal reflections recognized within a series of continuous inclined ones are interpreted as backset bedding, cut and fill (chutes) or slope failure structures (Roberts et al. 2003; Eilersten et al. 2011). Progradation of foresets towards the S-SSE is evident from the position of profiles (Fig. 9A). Comparison with the situation in the outcrop (Fig. 5A) where the transport direction was generally towards the NNE-NE points to the existence of several deltaic lobes. Deposits of GRU 4 are not outcropped. They have been interpreted either as FA 3 or as FA 4 and so also with respect to the results of the drillings in the close surrounding. Parallel reflections with a low, subhorizontal angle of dip which underlie the inclined reflections of the foreset are commonly interpreted as bottomset deposits of Gilbert deltas (Jol & Smith 1991; Eilersten et al. 2011). Locally observed lateral transition of steeply inclined reflections of GRU 3 into low-inclined reflections of GRU 4 (white arrows in Fig. 9D) can be interpreted as representing basinward transition of the foreset to the bottomset (Eilersten et al. 2011). They overlie the basal unconformity and show scoop-shaped scours (about 1 m deep and about 10 m wide). These structures resemble "spoon-shaped depressions" (Breda et al. 2007, 2009; Leszczyński & Nemec 2015) formed by turbidity currents descending a steep subaqueous slope and undergoing a hydraulic jump at its toe. However, sharp contact of gravels and underlying offshore mudstones of FA 4 is very common in the surrounding drill holes. Downlap of the inclined reflection of GRU 3 on the highly irregular top of GRU 4 with little preservation of their transition reveals prograding of the foreset on the eroded top of underlying beds. Variations in occurrence of the bottomset might also be partly attributed to the bedrock morphology.

Provenance analysis

Provenance analysis is based on the pebble petrography and analyses of heavy minerals.

Petrography and size of pebbles and cobbles, shape and roundness of pebbles

The gravels can be classified as polymict. Dominance of light beige, brown, grey, dark in colour, bituminous, micritic or bioclastic limestone and dolomite pebbles and cobbles is a typical feature. The content of carbonates usually varies between 30 % and 82.0 % (average/AVG 40.9 %). The cobbles or boulders of carbonates typically form the largest found extraclast (max. 65 cm) (Fig. 2D). Carbonate pebbles are mostly discs (38–49 %), less common are spheres (27–29 %), blade pebbles (16–22 %) or rods (8–15 %). Their average value of form ratio (Sneed & Folk 1958) varies between 0.27 and 0.43. The average value of sphericity (Sneed & Folk 1958) varies between 0.65 and 0.68 and average value of sphericity (Krumbein 1941 in Carver 1971) between 0.69 and 0.7. The average value of flatness ratio (Cailleux 1945 in Carver 1971) varies between 1.94 and 2.04. The average value of isometry index (Sarkisjan & Klimova 1955) varies between 1.02 and 1.04. The average elongation index (Folk 1965) is between 0.73 and 0.75 (equant). The average value of roundness index (Wentworth 1933 in Carver 1971) varies between 0.73 and 0.75 (well rounded).

Quartz pebbles are also quite common forming 4.4–49.9 % (AVG 18.4 %) of the pebble spectra. Various varieties of quartz are present. Whitish, milky quartz is the main one, with dark or light grey and pinkish types subordinating. Quartz pebbles are mostly discs (49 %), less common are spheres (19 %), blades (16 %) or rods (16 %) with maximum diameter dominantly between 1 and 5 cm. The average value of form ratio (Sneed & Folk 1958) of quartz pebbles is 0.39, and the average value of sphericity pebbles is 0.65 as defined by Sneed & Folk (1958) and 0.69 as defined by Krumbein (1941 in Carver 1971). Their average value of flatness ratio (as defined by Cailleux 1945 in Carver 1971) is 2.04. The average value of isometry index (Sarkisjan & Klimova

1955) is 1.01. The average elongation index (Folk 1965) is 0.74 (equant). The average value of roundness index (Wentworth 1933 in Carver 1971) is 0.74 (well rounded).

Sandstone pebbles (fine, middle or coarse-grained arkoses, greywackes, quartzose sandstones, calcareous sandstones) were identified in all samples, exceptionally forming up to 32.2 % of the pebble spectra (AVG 9.7 %). Presence of cherts (dark grey, brown or red brown) is typical, which can reach up to 11.9 % (AVG 10.4 %). A radiolarite pebble was described by Přichystal (2009). Typical occurrence of mudstone (silty clays) intraclasts can exceed 10 % of the pebble spectra, however their content is often difficult to quantify in relatively small drill cores. The intraclasts are typically significantly larger than the associated extraclasts and their size can sometimes reach over one metre in diameter (max. 3.5 m). Micropaleontological study of intraclasts (Švábenická & Čtyroká 1999; Petrová 2002) confirms the source mostly from the deposits of the Laa Fm. (Karpatian), less commonly from the Grund Fm. (Early Badenian) and canibalization of the older basin infill. Čtyroký (1993) connected the source of intraclasts with processes in the thrust front. Coal cobbles were recognized exceptionally (Nehyba et al. 2008).

Crystalline rocks in general form only the minor portion of the pebble suite; however, exceptionally, they can represent more than 30 % (AVG 8.2 %). Metamorphic rocks are a stable pebble component and are mostly represented by gneisses (up to 22 %), quartzites (up to 7.4 %) or mica schists (up to 11.9 %). Pebbles of magmatic rocks were described in the majority of samples forming up to 8.1 % (AVG 2.4 %). Two types of magmatites were recognized, namely granitic rocks (granites, granodiorites, aplites) and volcanic (melaphyre, diabase, rhyolites) rocks (similarly Přichystal 2009). Some differences in the content of individual rocks in the pebble spectra are influenced by varied grain size of the samples (outcrops vs. borehole cores).

Heavy minerals

Heavy minerals are sensitive indicators of the provenance, weathering, transport, deposition and diagenesis (Morton & Hallsworth 1994) especially if combined with the chemistry of selected heavy minerals (Morton 1984). The ZTR (zircon + tourmaline + rutile) index is widely accepted as a criterion for the mineralogical "maturity" of heavy mineral assemblages (Hubert 1962; Morton & Hallsworth 1994) in the case of derivation from a similar source. Garnet and rutile represent common heavy minerals in the studied deposits, being relatively stable in diagenesis and having a wide compositional range, thus enabling further evaluation in detail.

Heavy mineral assemblages

Garnet always dominates in the heavy mineral spectra and its content varies between 69.1 and 93.4 % (AVG 77.6 %). Zircon (0.5–11.9 %, AVG 5.4 %), represents the second most common mineral. Staurolite (0.7–5.2 %, AVG 6.0 %), rutile (0.3–8.2 %, AVG 4.3 %), disthene (0–6.4 %, AVG 3 %), apatite (0–7.0 %, AVG 2.6 %), tourmaline (0.2–6.0 %, AVG 1.5 %) and amphibole (0–8.5 %, AVG 0.1 %) represent accessory but relatively common heavy minerals. The presence of titanite, anatase, epidote, monazite, andalusite, pyroxene and sillimanite was rather exceptional. The heavy mineral assemblage can be mostly (89.5 %) described as garnet rarely (10.5 %) as garnet-zircon. The value of ZTR ranges between 1.9 and 11.8 (AVG 7.8).

Garnet

The chemistry of detrital garnet is widely used for the determination of provenance (Morton 1991).

The garnet composition was typical with its predominance of an almandine component. Ten garnet types (T1–T10) were determined in detail. The most common T1 forms 35.5 % of the garnet spectra and is represented by grossular–almandine garnets with a composition in the range $Alm_{58–78}Grs_{10–32}Prp_{3–9}Sps_{0–9}$. T2 forms 21.5 % and is composed by pyrope–almandine garnets with their typical composition in the range $Alm_{53–85}Prp_{11–45}Grs_{0–9}Sps_{0–8}$. T3 forms 20 % and is represented by grossular-almandine garnets with increased contents of pyrope and compositions of $Alm_{47–75}Grs_{13–30}Prp_{10–24}Sps_{0–5}$. T4 forms 6.5 % and is composed of almandine garnets with low contents of pyrope, grossular and spessartine components and the usual composition is in the range $Alm_{80–86}Prp_{5–9}Grs_{0–9}Sps_{1–9}$. T5 and T6 both equally form 5 % of the garnet spectra. T5 consists of pyrope–almandine garnets with increased grossular contents and the composition $Alm_{52–71}Prp_{12–20}Grs_{11–17}Sps_{0–2}$. T6 is represented by grossular–almandine garnets with an increased content of spessartine and a composition in the range $Alm_{65–66}Grs_{18–19}$ $Sps_{10–11}Prp_{4–5}$. T7 is represented by spessartine–almandine garnets with a composition of $Alm_{48–76}Sps_{14–38}Prp_{3–9}Grs_{3–8}$ and forms 4.8 %. T8 forms 2.5 % and is composed of spessartine–almandine garnets with an enriched grossular component and composition in the range $Alm_{58–72}Sps_{12–19}Grs_{10–17}Prp_{4–6}$. Both T9 and T10 are very rare and make up 0.5 % of the garnet spectra equally. T9 is represented by spessartine–almandine garnets with an increased content of pyrope and composition $Alm_{68}Sps_{15}Prp_{12}Grs_{4}$. T10 is composed of grossular-almandine garnets with an increased content of both pyrope and spessartine and composition Alm_{62} $Grs_{15}Sps_{11}Prp_{10}$.

Classification diagrams (Mange & Morton 2007; Aubrecht et al. 2009; Krippner et al. 2014) were used for evaluation of the potential primary sources. The PRP−ALM+SPS−GRS diagram (Mange & Morton 2007) in Figure 10A reflects the most important role (59.6 %) of garnets from amphibolite–facies metasedimentary rocks; significantly less common are garnets from intermediate to felsic igneous rocks (24.0 %) or garnets from high-grade granulite facies metasediments and intermediate felsic igneous rocks (12 %). Only garnets from high-grade mafic rocks are exceptional (4.4 %). The PRP–ALM–GRS diagram (Aubrecht et al. 2009) in Figure 10B indicates the most dominant (84.5 %) primary source of

garnets derived from gneisses and amphibolites metamorphosed under amphibolite-facies conditions. Garnets reflecting the source from gneisses or amphibolites metamorphosed under pressure and temperature conditions transitional to granulite- and amphibolite-facies metamorphism are not common (8.5 %), similarly to garnets derived from granulites (7.0 %).

The GRS–SPS–PRP diagram (Fig. 10C) allows comparison with possible source rocks along the eastern margin of the Bohemian Massif (Otava et al. 2000; Čopjaková et al. 2002, 2005; Čopjaková 2007; Buriánek et al. 2012). Some garnets can be compared to the Moravian Zone, the Moldanubicum, or the Brno Massif; however, they are commonly outside the diagnostic fields. The results are aligned with a noticeable lateral elongation in the PRP–GRS line. This distribution significantly differs from the distribution recognized for the Myslejovice Fm. of Moravian–Silesian Paleozoic (Culmian) deposits (Otava et al. 2000), where the source of Neogene deposits of the Carpathian Foredeep is commonly traced (Hladilová et al. 2014; Holcová et. al. 2015). The composed diagram (Fig. 11) allows comparison with garnets from Krosno and Ždánice–Hustopeče Fm. of the Western Carpathian Flysch Zone, which represents an active margin of the basin. Only part of the studied data fits with the diagnostic fields, however; commonly bi-lateral distribution of the results can be followed outside the diagnostic field.

Rutile

Rutile, which represents one of the most stable heavy minerals, is commonly used for provenance analyses (Force 1980; Zack et al. 2004a, b; Triebold et al. 2007).

The concentration of the main diagnostic elements (Fe, Nb, Cr and Zr) varies significantly in the studied samples. The concentration of Nb ranges between 388 and 5800 ppm (average 1854.7 ppm), the concentrations of Cr vary between 418 and 1998 ppm (average 418 ppm), of Zr between 50 and 5389 ppm (average 429 ppm), and the value of log Cr/Nb is mostly negative (76.5 %). The discriminate plot Cr vs. Nb (Fig. 12) shows two different trends in the rutile provenance

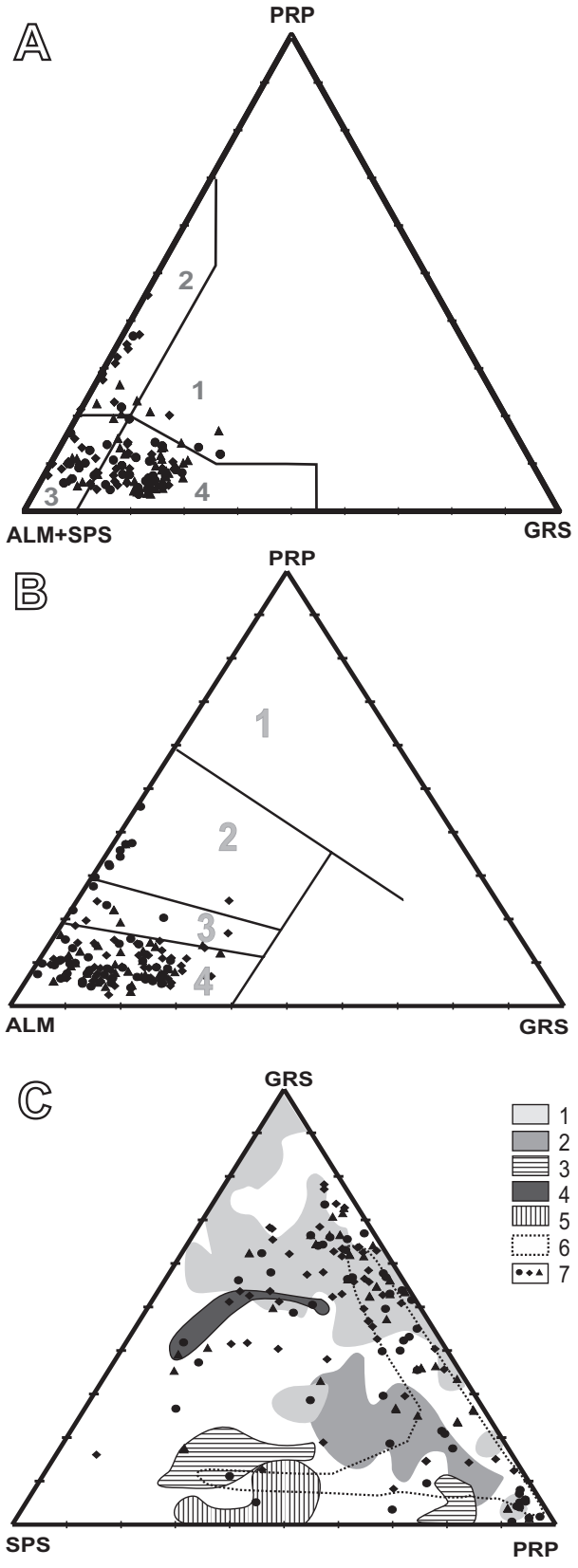

Fig. 10. Ternary diagrams of the chemistry of detrital garnets (ALM — almandine, GRS — grossular, PRP — pyrope, SPS — spessartine). **A** — Discrimination diagram according to Mange and Morton (2007) (1– pyroxenes and peridotites, 2 – high-grade granulite facies metasediments and intermediate felsic igneous rocks, 3 – intermediate to felsic igneous rocks, 4 – amphibolite facies metasedimentary rocks); **B** — Discrimination diagram according to Aubrecht et al. (2009) (1 – pyroxenes and peridotites, 2 – felsic and intermediate granulites, 3 – gneisses and amphibolites metamorphosed under pressure and temperature conditions transitional to granulite and amphibolite facies metamorphism, 4 – gneisses metamorphosed under amphibolite facies conditions); **C** — Ternary diagram of the chemistry of detrital garnets in comparison with possible source areas (1 – the Moravian Zone, 2 – the Moldanubicum, 3 – the Svratka Crystalline Complex, 4 – granites of the Brno Massif, 5 – migmatites of the Brno Massif, 6 – younger part of the Moravian–Silesian Palaeozoic/Culmian, 7 – samples from studied coarse-grained deltas). Data from source rocks according to Otava et al. (2000); Čopjaková et al. (2002, 2005); Čopjaková (2007) and Buriánek et al. (2012).

well. The majority of rutiles originated from metapelitic rocks (64.7 %), whereas origins from metamafic rocks (23.5 %) or pegmatites (11.8 %) are less common. The Zr-in-rutile thermometry of metapelitic zircons only (see Zack et al. 2004a, b; Meinhold et al. 2008) indicates that 58.8 % of these metapelitic rutiles belong to green schist metamorphic facies and 41.2 % to the amphibolite/eclogite facies. The calculated temperatures range between 246–753 °C (equation Zack et al. 2004b) showing the significant role of low-medium temperature metamorphic rocks in the source area. The diagnostic criteria of Triebold et al. (2012) confirm prevailing provenance from metapelites (61.8 %) over metamafic sources (26.5 %).

These results differ from the data known for the Karpatian or the Lower Badenian deposits of the Carpathian Foredeep (Francírek & Nehyba 2016; Nehyba et al. 2016) and indicate a different provenance of rutile in this case.

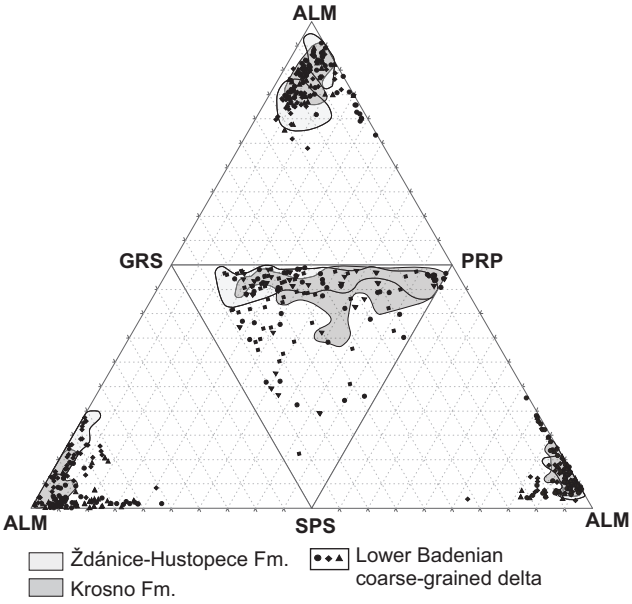

Fig. 11. Ternary diagram of the chemistry of the detrital garnets and comparison with garnets from Krosno and Ždánice–Hustopeče Fm. of the Western Carpathian Flysch Zone (ALM – almandine, GRS – grossular, PRP – pyrope, SPS – spessartine).

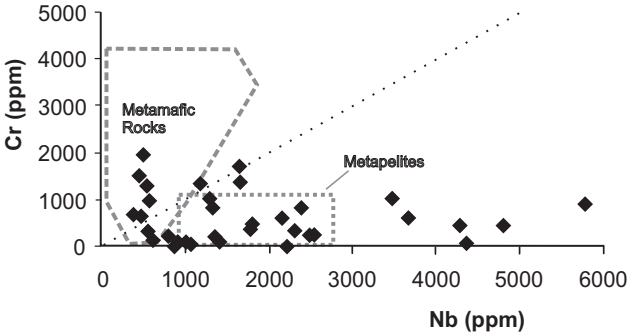

Fig. 12. Discrimination plot of Cr vs. Nb of investigated rutiles.

Interpretation of the provenance data

Polymict gravels with a dominance of Mesozoic carbonates, broad spectra of further sedimentary rocks, and a content of magmatic and metamorphic rocks all point to sources in the Alpine–Carpathian orogene (cf. Nehyba & Roetzel 2004; 2011). The high similarity in shape characteristics and well roundness of both carbonate and quartz pebbles reveal multiple sources and the role of redeposition. Abundant intraformational clasts suggest enhanced erosion of subaerially exposed distal offshore deposits (both Karpatian schlier and Lower Badenian tegel), significant relative sea-level fall, large-scale slope failures during deposition and attendant sediment gravity flow processes.

The heavy mineral assemblage is very typical for the Lower Badenian deposits of the Carpathian Foredeep. The dominant presence of garnet confirms the important role of metamorphic complexes (crystalline schists) in the source area. Zircon, tourmaline and rutile are common in acidic to intermediate magmatic rocks, as in selected metamorphic rocks (von Eynatten & Gaupp 1999) or can be connected with redeposition from older deposits. The relatively stable heavy mineral assemblage together with low and varied content of low-stabilty heavy minerals (apatite, pyroxene, amfibole etc.) point to relatively weathered rocks in the primary source area, formed by both crystalline schists and magmatic rocks (a mature continental crust). Low values of ZTR index are typical for immature clastic deposits with a relatively low role of recycling (or significant role of carbonates in the source area).

Dominance of almandine garnets is a very common feature of the garnet spectra in the deposits along the eastern margin of the Bohemian Massif. These are recognized in the Moravian–Silesian Paleozoic (Culmian) rocks (Otava et al. 2000; Čopjaková et al. 2002, 2005; Čopjaková 2007), Permo–Carboniferous deposits (Nehyba et al. 2012; Nehyba & Roetzel 2015), Jurassic deposits of both the Gresten and Nikolčice Formations (Nehyba & Opletal 2016; 2017), Paleogene deposits of the Western Carpathian Flysh Zone (Otava 1998; Otava et al. 1997; Stráník et al. 2007), and also in Eggenburgian and Ottnangian, Karpatian (Francírek & Nehyba 2016) and Lower Badenian (Nehyba et. al. 2016) deposits of the Carpathian Foredeep itself. However, the distribution of recognized garnet types varies within these deposits. Obtained garnet data can to some extent be compared either with the results from the depositional unit III of Karpatian deposits (Francírek & Nehyba 2016), or with the Lower Badenian deposits along the marginal flank of the crystalline basement (Nehyba et al. 2016). However, here also the studied garnet spectra differ in detail. The occurrence of spessartine–almandine garnets (T 7–9) is remarkable and signifies a source from the crystalline rocks of the basement, because such garnets are generally very common in the gneisses, migmatites and mica schists of the Bohemian Massif (Čopjaková 2007; Francírek & Nehyba 2016). A direct source from the passive margin of the basin formed by crystalline rocks of the Bohemian Massif is highly improbable due to the

basin configuration, position of the studied deposits in the basin and the depositional environment of the studied deposits. Both diagrams (Fig. 10A,B) reveal the dominance of the garnets from amphibolites and metamorphosed rocks of amphibolite facies and a relatively uniform primary source.

The obtained provenance data can be summarized: 1) The provenance of the gravels is specific and partly differs from the known data from the sedimentary infill of the Carpathian Foredeep. 2) Several partial sources can be recognized: a) provenance from Mesozoic carbonates of the Alpine–Carpathian orogeny, b) crystalline rocks of the eastern margin of the Bohemian Massif, c) older sedimentary infill of the Carpathian Foredeep and/or Alpine Molasse Zone, and d) sedimentary rocks of the Carpathian Flysch Zone. The role of these sources varies in individual samples (see the common bilateral distribution of garnet data in diagrams). A source from an area now below the surface is highly probable.

The composition of garnet, rutile and also pebble petrography of the deposits studied significantly differs from similar data obtained for the autochthonous Jurassic beds along the eastern margins of the Bohemian Massif (Nehyba & Opletal 2016, 2017). This result indirectly challenges the provenance of carbonate pebbles only from Jurassic beds (see Eliáš 1981; Řehánek 2001). Part of the carbonates could originate from older Triassic carbonate units of the Northern Calcareous Alps (similarly Přichystal 2009). Several authors (Menčík 1973; Eliáš 1981; Stráník et al. 1999; Řehánek 2001) supposed the source to be from autochthonous (subsurface) Jurassic deposits of the SE margin of the Bohemian Massif. However, a detailed microfacies and provenance study of these carbonates is missing.

Discussion

The creation of an adequate initial bathymetry and topography necessary for the initiation of deposition of Gilbert delta foresets is connected with the formation of a significant basinward dip of the depositional slope (Postma 1990). So, especially KSS 1 and partly also KSS 8 are interpreted as the result of a significant fall in base level. Further Gilbert delta growth requires: (i) a high sediment supply; (ii) high water flux; and (iii) high creation of accommodation space (Postma 1990). Deposition of both D1 and D2 reveals a general increase of bathymetry. The sedimentary record of D1 and D2 is dominated by large-scale prograding and aggrading topset and foreset packages which mainly record the creation and fill of available accommodation space. Such stratigraphic architecture reflects a low and gradual rate of creation of accommodation space. As the delta records essentially vertical stacking of gravel beds, and as the proportion of fine-grained facies is very low, the distal part of the basin was never filled by deltaic deposition and the basin gradually deepened with time, thus allowing foreset heights to increase (Backert et al. 2010). Sea-level rise corresponds to rapid transgression across the D1 delta top (KSS 7) and termination of deltaic deposition in the study area. Similarly also the termination of D2 (KSS 10) could be connected with transgression as a transgressive surface, however it could also represent the flooding surface due to smaller scale of D2 delta. Hypothetical reconstruction of the depositional setting during the evolution of both the lower delta D1 and upper delta D2 are presented in Fig. 13.

The dimensions of the studied Gilbert deltas can be partly compared with the data in literature, taking into account dating of their development. Backert et al. (2010) estimated that a giant Gilbert-type delta (thickness >600 m) was deposited during a period of 500 to 800 ky. Breda et al. (2007) supposed that steep dipping clinoforms 50 to 250 m thick were formed during 4th-order (0.2–0.5 Ma) cycles. Similarly Benvenuti (2003) estimates that the evolution of a 20 m coarse-grained delta took about 100 ky. According to Gobo et al. (2015) a Gilbert delta about 100 m thick formed during approx. 50 ky. Significantly more rapid constructions of deltas were documented by Corner (2006) and Eilertsen et al. (2011) who reported coarse-grained deltas about 60 m thick formed during less than 10 ky. Similarly Postma & Cruickshank (1988) documented prograding of Gilbert type delta about 15 m thick during approx. 2 ky. Likewise Rhine & Smith (1988) described approx. 20 m thick coarse-grained delta deposited during a time period of 1700 years. Even more rapid formation was documented by Plink-Björklund & Ronnert (1999), who described a coarse deltaic clastic wedge 20–80 m thick deposited during a period of about 100 years. Similarly Nehyba et al. (2017) documented progradation of about 4 m thick Gilbert delta during less than 20 years. Although there is no simple positive correlation between the time period of delta formation and volumetry/scale of deltaic body it is obvious that D1 and D2 have different scales. Similarly, although the evidence of two laterally and stratigraphically separated coarse-grained Gilbert deltas indicate two cycles of sea-level change, these cycles could have different regional/basin extent/significance and could be of different orders (3rd vs. 4th order). However, different paleoslope or variations in the ratio of water/sediment discharge can also affect the scale and distribution of the coarse grained deltaic deposits. With a high ratio of water/sediment discharge, the feeder system is likely to be a sheet flow that can aggrade more uniformly along the shoreline. As the ratio of water/sediment discharge decreases, the stream channel sedimentation becomes dominant, and also the lateral mobility of the feeder flow is reduced (Muto & Steel 2001).

The deep scours/KSS 1 and 8 that occur at the bases of the Gilbert deltas D1 and D2 successions are interpreted as sequence boundaries/regressive surfaces of fluvial erosion. They are results of forced regression and relative sea level fall (downstepping, sediment by-pass, basinward shift of facies belt, negative accommodation). More extended basinward progradation, deeper incision and larger thickness point to more pronounced sea-level fall during the formation of KSS 1 then KSS 8.

The sedimentary infill (or its substantial part) of studied Gilbert deltas is connected with ongoing normal regression, which is typified by the rate of accommodation lower than

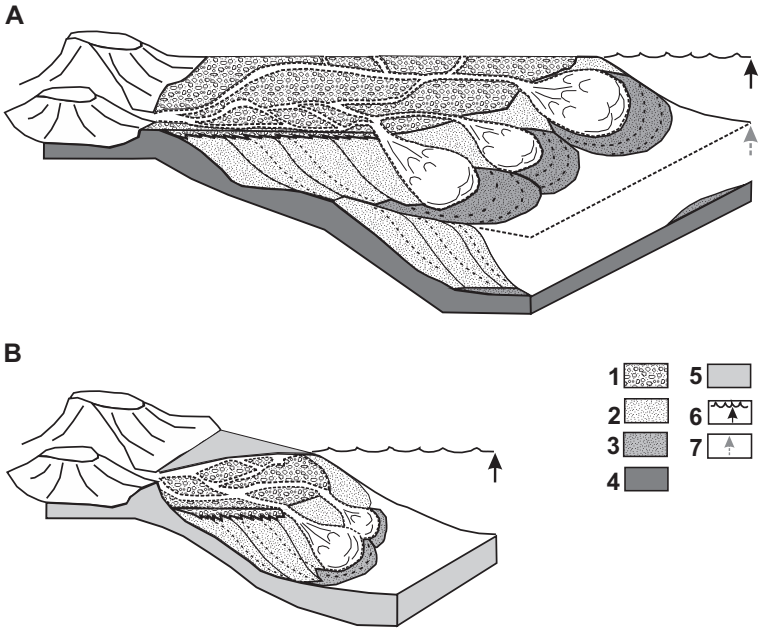

Fig. 13. Schematic model of the deposition condition of the lower Gilbert delta (**A**) and upper Gilbert delta (**B**) (1 — topset deposits, 2 — foreset deposits, 3 — bottomset deposits, 4 — older basin infill/mostly Karpatian in age, 5 — older basin infill/mostly Lower Badenian in age, 6 — sea level, 7 — former position of sea level).

the sediment supply. In such circumstances prograding and aggrading foresets thicken downdip, dominant progradation driven by sediment supply is followed with some aggradation. Moreover, whereas the rates of progradation decrease with time, the rates of aggradation increase with time (as a result of accelerating relative sea level rise). This situation is reflected by the stacked retrograding pattern of deltaic clinoforms in the northern branch of D1. The sedimentary infills are capped by transgressive surfaces.

The differences in the stratigraphic architecture of the northern and southern branch of D1 could have resulted from predisposed paleotopography (by incision) and paleobathymetry of the basin floor and/or local variation of sediment supply effecting on A/S ratio.

Two almost coeval coarse-grained Gilbert deltas documented in the depositional succession of the Western Carpathian Foredeep basin reflect two base level cycles/sequences probably of different scale. However, deltas D1 and D2 could also represent two different Early to Middle Miocene 3rd order cycles, namely TB 2.3. and TB 2.4. (Kováč et al. 2004; Hohenegger et al. 2014). Moreover, two scales of base level cycles were recognized in the depositional succession of lower D1 delta. Such a complex state represents a complication for the basin lithostratigraphy. Recognition of a longer-term cycle (probably 3rd order cycle TB 2.3. sensu Haq et al. 1988) and high-frequency cycles (4th to 5th order) constitute a challange for the further research in the Western Carpathian Foredeep basin. Adequate biostratigraphical and lithostratigraphical correlations of the Early Badenian sedimentary succession within the Carpathian Foredeep and the Alpine Molasse Basin based on facies architecture of marginal and basinal facies are necessary to understand the actual role of local and regional ruling factors and the establishment of reliable sequence stratigraphy of Early to Middle Miocene deposits.

Two Lower Badenian gravel beds (13 and 15 m thick) separated by an about 77 m thick interbed of fine sands and silty shales were also recognized in the Roggendorf-1 borehole (see Fig. 1) drilled in the Early to Middle Miocene deposits of the Alpine–Carpathian Foredeep approx. 40 km SW of the area under study (Ćorić & Rögl 2004). Both gravels contain abundant limestone and dolomite pebbles which originated from the Calcareous Alps and Flysch Unit. The boundary between zones NN4 and NN5 was observed within the fine-grained interbed. The basal gravels are regarded as the transgressive base of the Badenian in the Molasse Basin north of the Danube (Ćorić & Rögl 2004). The upper gravels are considered to be the coarse basal transgression level of the Grund Formation. Remarkable similarity in petrography and stratigraphic position might point to a link between these gravel beds and D1+D2 deposits as a response to adequate factors/processes affecting the basin architecture. However, such a simple link might be misleading. Coarse-grained Gilbert deltas are highly prone to rapid changes in basin configuration, sea-level, climate and sediment supply during the evolution of the system (Nemec 1990a; Postma 1990) as a result of dynamic equilibrium between sediment supply, basin energy conditions, accommodation and the overall geological framework.

The studied Gilbert deltas represent infill of two incised-valley systems as defined by Zaitlin et al. (1994). The configuration of the alluvial feeder system has a crucial influence on the gross geometry of deltas (Postma & Roep 1985; Kim & Chough 2000). The scale (lateral extent and thickness) of deltaic deposits, incised base and provenance analyses all point to an extensive fluvial system with a large catchment basin. Sediment and water flux in this fluvial system would therefore reflect regional tectonics and climatic variations. The very similar provenance of D1 and D2 joined both deltas into a common fluvial system. Jiříček (2002) supposed that the partially comparable Matzen delta in the Vienna basin was formed by a Badenian Paleo-Danube. The position of the fluvial entry into the basin implies incised valley/valleys formed within the active basin margin (wedge-top) oriented perpendicularly to oblique to the foredeep part of the foreland basin. This allochthonous part of the basin is not preserved or does not outcrop. Tectonic predisposition of such a valley (available morphology of the piggy-back sub-basin?) is probable. It is also possible that the fluvial system was initially oriented in the NNE–SSW direction (the axis of the flexure and the basin). The tectonic setting at the margin of a thrust belt and morphology of adjacent parts of the Waschberg–Ždánice unit

(accelerated by a sea-level drop) diverted the drainage into a western direction. Further tectonic activity finally switched the drainage system towards the east into the subsiding and opening Vienna Basin.

Conclusions

The Lower Badenian "basal or marginal coarse clastics" in the southernmost part of the Western Carpathian Foredeep were interpreted as deposits of two coarse-grained Gilbert deltas based on the study of both outcrops and boreholes.

Four facies associations/principal depositional environments have been identified in the studied deposits. Three of them correspond to a tripartite Gilbert type delta profile. Facies association 1 is interpreted as topset, facies association 2 as foreset and facies association 3 as bottomset. The remaining FA 4 represents open marine pelagic deposits.

The lower delta is significantly thicker (up to 160 m), more areally extended and reveals a more complicated stratigraphic architecture than the upper delta. The laterally traceable boundary/base of the lower Gilbert delta is connected with a significant migration of basin depocentre, a new basin physiography with relatively steep margins, which is interpreted as a consequence of a relative sea level fall, followed by major erosion and incision several tens of m downward and several km basinward. This surface represents a sequence boundary and is also arbitrarily used as the Karpatian/Badenian boundary. Formation, progradation and aggradation of the thick coarse-grained Gilbert delta pile generally indicate a dramatic increase of sediment supply from the hinterland, followed by both relatively continuous sediment supply and an increase of accommodation space over the available time (interpreted as lowstand normal regression). Two coeval deltaic branches were recognized in the lower delta with partly different stratigraphic arrangements (directed by the interplay between the available accommodation space and the sediment supply), confirmed by identified key stratal surfaces. The northern delta branch is typical with generally uniform lithology and reflects delta progradation, aggradation and final retrogradation. The southern branch is characterized by a more complicated lithology due to multiple alternation of facies associations and a slightly higher total thickness. Such an arrangement points to alternation of phases of delta progradation and retrogradation (followed by aggradation). The differences in the stratigraphic architecture of the branches are explained by variations in the sediment delivery, inherited paleotopography and by a possibly relatively more rapid formation of accommodation space towards the southern part of the basin. Termination of deposition of the lower delta is connected with relatively rapid and extended drowning of the delta plain and is explained by a transgressive event (Lower Badenian in age).

The upper delta was recognized only in a restricted area and its maximum total thickness reaches 33 m. The lower boundary of this delta reflects a significant decrease in the ratio of accommodation space/sediment supply, which is interpreted as a relative sea level fall and a sequence boundary (within the Lower Badenian). Subsequent progradation and aggradation of coarse-grained Gilbert delta deposits is connected with a following increase of accommodation space and intense, spatially localized sediment supply. The flat upper surface of this Gilbert delta is connected with a landward shift in the topset breakpoint and rapid flooding (all Lower Badenian in age).

Lateral and vertical/stratigraphical separation of both Gilbert deltas suggests migration of the delta depocentre and evolution of the basin margin. The evidence of two laterally and stratigraphically separated coarse-grained Gilbert deltas indicates two regional/basin wide sea-level cycles/depositional sequences, but not necessarily of the same order.

Provenance analysis did not recognize significant differences between the deposits of the two Gilbert deltas, but revealed their multiple sources and the role of basin cannibalism. The studied gravels are polymict with a dominant role of Mesozoic carbonates, which make them specific in the sedimentary infill of the Carpathian Foredeep. Although the heavy mineral assemblage of the studied deposits is very typical for the Lower Badenian deposits of the Carpathian Foredeep, the garnet spectra differ in detail from available data from the basin. The provenance analysis identified several partial source areas (Mesozoic carbonates of the Northern Calcareous Alps and/or the Western Carpathians, crystalline rocks of the eastern margin of the Bohemian Massif, older sedimentary infill of the Carpathian Foredeep and/or Alpine Molasse Zone, sedimentary rocks of the Carpathian/the Alpine Flysch Zone). A source from an area now below the surface is highly probable. The scale (lateral extent and thickness) of deltaic deposits, their deeply incised base and provenance all point to an extensive fluvial system with large catchment basin.

Acknowledgements: The manuscript highly benefited from thoughtful reviews of two unknown reviewers. The author also thanks the Czech Geological Survey for giving access to the Iváň 1 and 22-41 D Pasohlávky boreholes.

References

Aubrecht R., Méres Š., Sýkora M. & Mikuš T. 2009: Provenance of the detrital garnets and spinels from the Albian sediments of the Czorsztyn Unit (Pieniny Klippen Belt, Western Carpathians, Slovakia). *Geol. Carpath.* 60**,** 463–483.

Backert N., Ford M. & Malartre F. 2010: Architecture and sedimentology of the Kerinitis Gilbert-type fan delta, Corinth Rift, Greece. *Sedimentology* 57, 2, 543–586.

Beaumont C. 1981: Foreland basins. *Geoph. Journal of the Royal Astronomical Society* 55, 291–329.

Benvenuti M. 2003: Facies analysis and tectonic significance of lacustrine fan-deltaic successions in the Pliocene-Pleistocene Mugello Basin, Central Italy. *Sediment. Geol.* 157, 197–234.

Blum M.D. & Törnquist T.E. 2000: Fluvial responses to climate and sea-level change. A review and look forward. *Sedimentology* 47, S1, 2–48.

Breda A., Mellere D. & Massari F. 2007: Facies and processes in a Gilbert-delta-filled incised valley (Pliocene of Ventimiglia, NW Italy). *Sediment. Geol*. 200, 31–55.

Breda A., Mellere D., Massari F. & Asioli, A. 2009: Vertically stacked Gilbert-type deltas of Ventimiglia (NW Italy): the Pliocene record of an overfilled Messinian incised valley. *Sediment. Geol*. 219, 58–76.

Brzobohatý R. & Cicha I. 1993: Carpathian Foredeep. In: Přichystal A., Obstová V. & Suk M.: Geology of Moravia and Silesia. *MZM, PřF MU*, 123–128 (in Czech with English abstract).

Brzobohatý R. & Stráník Z. 2011: Paleogeography of the Early Badenian connection between the Vienna Basin and the Carpathian Foredeep. *Central European Journal of Geosciences* 4, 1, 126–137.

Buriánek D., Tomanová Petrová P. & Otava J. 2012: Where is the source of the clastic deposits of Miocene deposits in the surroundings of Brno? *Acta Musei Moraviae, Scientae geologicae* 97, 153–166 (in Czech with English abstract).

Carver R.E. 1971: Procedures in Sedimentary petrography. *John Wiley & Son*, New York, 1–653.

Chough S.K. & Hwang I.G. 1997: The Duksung fan delta, SE Korea: growth of delta lobes on a Gilbert-type topset in response to relative sea-level rise. *J. Sediment. Res*. 67, 725–739.

Colella, A. 1988: Pliocene-Holocene fan deltas and braid deltas in the Crati Basin, southern Italy: a consequence of varying tectonic conditions. In: Nemec W. & Steel R.J. (Eds.): Fan Deltas: Sedimentology and Tectonic Settings. *Blackie*, London, 50–74.

Collinson J., Mountney N. & Thompson D. 2006: Sedimentary Structures, *Terra Publishing*, Harpenden, Hertfordshire, England, 1–292.

Čopjaková R. 2007: The reflection of provenance changes in the psefitic and psamitic sedimentary fraction of the Myslejovice Formation (heavy mineral analysis). *Doctoral thesis*, *Masaryk University*, Brno, 1–137 (in Czech).

Čopjaková R., Sulovský P. & Otava J. 2002: Comparison of the chemistry of detritic pyrope-almandine garnets of the Luleč Conglomerates with the chemistry of granulite garnets from the Czech Massif. *Geologické výzkumy na Moravě a ve Slezku v roce 2001,* Brno, 44–47 (in Czech).

Čopjaková R., Sulovský P. & Paterson, B.A. 2005: Major and trace elements in pyrope–almandine garnets as sediment provenance indicators of the Lower Carboniferous Culm sediments, Drahany Uplands, Bohemian Massif. *Lithos* 82, 51–70.

Ćorić S. & Rögl F. 2004: Roggendorf-1 borehole, a key-section for Lower Badenian transgressions and the stratigraphic position of the Grund Formation (Molasse Basin, Lower Austria). *Geol. Carpath*. 55, 2, 165–178.

Corner G.D. 2006: A transgressive-regressive model of fjord valley fill: stratigraphy, facies and depositional controls. In: Dalrymple R.W., Leckie D.A. & Tillman R.W. (Eds.): Incised Valleys in Time and Space. *SEPM Spec. Publ.* 85, 161–178.

Čtyroký P. 1993: New data to Miocene stratigraphy on the map 34-23 Břeclav. *Zpr. geol. výzk. v roce 1992*, Prague, 18–21 (in Czech).

Dart C.J., Collier R.E.L., Gawthorpe R.L., Keller J.V.A. & Nichols G. 1994: Sequence stratigraphic of (?) Pliocene-Quaternary synrift, Gilbert-type fan deltas, northern Peloponnesos, Greece. *Mar. Petrol. Geol*. 11, 545–560.

DeCelles P.G. & Cavazza W. 1999: A comparison of fluvial megafans in the Cordilleran (Upper Cretaceous) and modern Himalayan foreland basin systems. *Geol. Soc. Am. Bull*. 111, 1315–1334.

DeCelles P.G. & Giles K. A. 1996: Foreland basin systems. *Basin Research* 8, 105-123.

Dellmour R. & Harzhauser M. 2012: The Iváň Canyon, a large Miocene canyon in the Alpine-Carpathian Foredeep. *Mar. Petrol. Geol*. 38, 83–94.

Doláková N., Brzobohatý R., Hladilová Š. & Nehyba S. 2008: The red-algal facies of the Lower Badenian limestones of the Carpathian Foredeep in Moravia (Czech Republic). *Geol. Carpath*. 62, 2, 133–146.

Eilertsen R.S., Corner G.D., Aasheim O. & Hansen L. 2011: Facies characteristics and architecture related to palaeodepth of Holocene fjord-delta sediments. *Sedimentology* 58, 1784–1809.

Ékes C. & Friele P. 2003: Sedimentary architecture and post-glacial evolution of Cheekye fan, southwestern British Columbia, Canada. In: Bristow C.S. & Jol H.M. (Eds.): Ground Penetrating Radar in Sediments. *The Geological Society London*, Bath, UK, 87–98.

Eliáš M. 1981: Facies and paleogeography of the Jurassic of the Bohemian Massif. *Sborník geol. Věd, Geol*. Praha, 35, 75–144.

Folk R.L. 1965: Petrology of sedimentary rocks. *Hemphill´s*, 1–159.

Force E.R. 1980: The provenance of rutile. *J. Sediment. Res*. 50, 485–488.

Ford M., Williams E.A., Malartre F. & Popescu S.M. 2007: Stratigraphic architecture, sedimentology and structure of the Vouraikos Gilbert-type fan delta, Gulf of Corinth, Greece. In: Nichols G., Williams E. & Paola C. (Eds.): Sedimentary Processes, Environments and Basins. A Tribute to Peter Friend. *Int. Assoc. Sedimentol. Spec. Publ*. 38, 49–90.

Francírek M. & Nehyba S. 2016: Evolution of the passive margin of the peripheral foreland basin: an example from the Lower Miocene Carpathian Foredeep (Czech Republic). *Geol. Carpath*. 67, 1, 39–66.

Gawthorpe R.L. & Colella A. 1990: Tectonic controls oncoarse-grained delta depositional systems in rift basins. In: Collela A. & Prior D.B. (Eds.): Coarse-Grained Deltas. *Int. Assoc. Sedimentol. Spec. Publ*. 10, 113–127.

Gilbert G.K. 1885: The topographic features of lake shores. *Ann. Rep. U.S. geol. Survey*. 5, 69–123.

Gobo K., Ghinassi M. & Nemec W. 2015: Gilbert-type deltas recording short-term base-level changes: Delta-brink morphodynamics and related foreset facies. *Sedimentology* 62, 1923–1949.

Haq B.U., Hardenbol J. & Vail P.R. 1988: Mesozoic and Cenozoic chronostratigraphy and cycles of sea-level change. In: Wilgus C.K., Hastings B.S., Kendall C.G.S.C., Posamentier H.W., Ross C.A., Van Wagoner J.C. (Eds.): Sea-level Changes: An Integrated Approach. *SEPM Spec. Publ*. 42, 71–108.

Hartley A.J., Weissmann G.S., Nichols G.J. & Warwick G.L. 2010: Large distributive fluvial systems: characteristics, distribution, and controls on development. *J. Sediment. Res*. 80, 167–183.

Hladilová Š., Nehyba S., Zagoršek K., Tomanová-Petrová P., Bitner M.A. & Demeny A. 2014: Early Badenian transgression on the outer flank of Western Carpathian foredeep, Hluchov area, Czech Republic. *Annales Societatis Geologorum Poloniae*, 84, 3, 259–279.

Hohenegger J., Ćorić S. & Wagreich M. 2014: Timing of the Middle Miocene Badenian Stage of the Central Paratethys. *Geol. Carpath*. 65, 1, 55–66.

Holcová K., Brzobohatý R., Kopecká J. & Nehyba S. 2015: Reconstruction of the unusual Middle Miocene (Badenian) palaeoenvironment of the Carpathian Foredeep (Lomnice/Tišnov denudational relict, Czech Republic). *Geol. Quarterly*. 59, 4, 654–678.

Hubert J.F. 1962: A zircon-tourmaline-rutile maturity index and the interdependence of the composition of heavy mineral assemblages with the gross composition and texture of sandstones. *J. Sediment. Petrol*. 32, 440–450.

Jervey M.T. 1988: Quantitative Geological Modeling of Siliciclastic Rock Sequences and their Seismic Expression. In: Wilgus K.W., Posamentier H., Hastings B.S., van Wagoner J., Ross C.A. & Kendall C.G.St.C. (Eds.): Sea-level Changes: An Integrated Approach. *Society of Economic Paleontologists and Mineralogists Spec. Publ.* 42, 47–69.

Jiříček R. 2002: The Evolution of the Molasse in the Alpino-Carpathian Foredeep and the Vienna Basin. EGRSE, *International Journal of Exploration Geophysics*, *Remote Sensing and Environment* 9, 1–2, 4–178 (in Czech).

Jol H.M. & Smith D.G. 1991: Ground penetrating radar of northern lacustrine deltas. *Can. J. Earth Sci*. 28, 1939–1947.

Kim J.W. & Chough S.K. 2000: A gravel lobe deposit in the prodelta of the Doumsan fan delta (Miocene), SE Korea. *Sediment. Geol*. 130, 183–203.

Kováč M., Baráth I., Harzhauser M., Hlavatý I. & Hudáčková N. 2004: Miocene depositional systems and sequence stratigraphy of the Vienna basin. *Cour. Forsch.-Inst. Senckenberg* 246, 187–212.

Krippner A., Meinhold G., Morton A.C. & von Eynatten H. 2014: Evaluation of garnet discrimination diagrams using geochemical data derived from various host rocks. *Sediment. Geol*. 306, 36–52.

Krystek I. 1974: Výsledky sedimentologického výzkumu sedimentů spodního bádenu v karpatské předhlubni (na Moravě). *Folia Univ. Purkyn. Brün. Geol.* Brno, 15, 8.

Kryštofová E. 2007: An Important Afuifer of Lower Badenian Clastic Sediments in Carpathian Foredeep. *Scripta Fac.Sci. Nat. Univ. Masaryk. Brunn., Geology*, 36, 73–75.

Lee S.H. & Chough S.K. 1999: Progressive changes in sedimentary facies and stratal patterns along the strike-slip margin, northeastern Jinan Basin (Cretaceous), southwest Korea: implications for differential subsidence. *Sediment. Geol*. 123, 81–102.

Leszczyński S. & Nemec W. 2015: Dynamic stratigraphy of composite peripheral unconformity in a foredeep basin. *Sedimentology* 62, 645–680.

Lowe D.R. 1982: Sediment gravity flows: II. Depositional models with special reference to the deposits of high-density turbidity currents. *J. Sediment. Petrol*. 52, 279–297.

López-Blanco M., Marzo M. & Piña J. 2000: Transgressive–regressive sequence hierarchy of foreland, fan-delta clastic wedges (Montserrat and Sant Llorenç del

Munt, Middle Eocene, Ebro Basin, NE Spain). *Sediment. Geol.* 138, 41–69.

Mange M.A. & Morton A.C. 2007: Geochemistry of heavy minerals. *Developments in Sedimentology* 58, 345–391.

Martini I., Ambrosetti E. & Sandrelli F. 2017: The role of sediment supply in large-scale stratigraphic architecture of ancient Gilbert-type deltas (Pliocene Siena-Radicofani Basin, Italy). *Sediment. Geol*. 350, 23–41.

Martinsen O., Ryseth A., Helland-Hansen W., Flesche H., Torkindsen G. & Idil S. 1999: Stratigraphic base level and f luvial architecture: Ericson Sandstone (Campanian), Rock Springs Uplift, SW Wyoming, USA. *Sedimentology* 46, 235–259.

Massari F. & Parea G.C. 1990: Wave–dominated Gilbert–type gravel deltas in the hinterland of the Gulf of Taranto (Pleistocene, southern Italy). In: Colella A. & Prior D.B. (Eds.): Coarse–Grained Deltas. *Int. Assoc. Sedimentol. Spec. Publ.* 10, 311–331.

Meinhold G., Anders B., Kostopoulos D. & Reischmann T. 2008: Rutile chemistry and thermometry as provenance indicator: An example from Chios Island, Greece. *Sediment. Geol*. 203, 98–111.

Menčík E. 1973: Contact of the Bohemian Massif and the West Carpathians Mts. In: Guide to excursion of X Congress of Carpathian-Balkan Geological Association. Bratislava, 1–30.

Miall A.D. 1996: The Geology of Fluvial Deposits: Sedimentary Facies, Basin Analysis, and Petroleum Geology. *Springer-Verlag*, Berlin, 1–582.

Morton A.C. 1984: Stability of detrital heavy minerals in Tertiary sandstones from the North Sea Basin. *Clay Miner.* 19, 287–308.

Morton A.C. 1991: Geochemical studies of detrital heavy minerals and their application to provenance research. In: Morton A.C.,Todd S.P. & Haughton P.D.W. (Eds.): Developments in Sedimentary Provenance Studies. *Geol. Soc. London, Spec. Publ*. 57, 31–45.

Morton A.C. & Hallsworth C.R. 1994: Identifying provenance-specific features of detrital heavy mineral assemblages in sandstones. *Sediment. Geol*. 90, 241–256.

Mulder T. & Alexander J. 2001: The physical character of subaqueous sedimentary density flows and their deposits. *Sedimentology* 48, 269–299.

Muto T. & Steel R.J. 1992: Retreat of the front in a prograding delta. *Geology* 20, 967–970.

Muto T. & Steel R.J. 1997: Principles of regression and transgression: the nature of the interplay between accommodation and sediment supply. *J. Sediment. Res*. 67, 994–1000.

Muto T. & Steel R.J. 2001: Autostepping during the transgressive growth of deltas: results from flume experiments. *Geology* 29, 771-774.

Mutti E., Tinterri R., Benevelli G., di Biase D. & Cavanna G. 2003: Deltaic, mixed and turbidite sedimentation ofancient foreland basins. *Mar. Petrol. Geol.* 20, 733–755.

Nehyba S. & Opletal V. 2016: Depositional environment and provenance of the Gresten Formation (Dogger) on the southeastern slopes of the Bohemian Massif (Czech Republic, subsurface data). Austrian J. Earth Sci. 109, 2.

Nehyba S. & Opletal V. 2017: Sedimentological study of the Nikolčice Formation — evidence of the Middle Jurassic transgression onto the Bohemian Massif (subsurface data).*Geol. Quarterly* 61, 1, 138–155.

Nehyba S. & Roetzel R. 2004: The Hollabrunn-Mistelbach Formation (Upper Miocene, Pannonian) in the Alpine-Carpathian Foredeep and the Vienna Basin in Lower Austria — An example of a Coarse-grained Fluvial System. *Jahrb. Geol. Bundesanst*. 144, 2, 191–221.

Nehyba S. & Roetzel R. 2011: Fluvial deposits of the St. Marein Freischling Formation insights into initial depositional processes on the distal external margin of the Alpine Carpathian Foredeep in Lower Austria. *Austrian J. Earth Sci.* 100, 2, 50–80.

Nehyba S. & Roetzel R. 2015: Depositional environment and provenance analyses of the Zobing Formation (Upper Carboniferous–Lower Permian), Austria. *Austrian J. Earth Sci.* 108, 2, 245–276.

Nehyba S. & Šikula J. 2007: Depositional architecture, sequence stratigraphy and geodynamic development of the Carpathian Foredeep (Czech Republic). *Geol. Carpath*. 58, 1, 53–69.

Nehyba S., Roetzel R. & Adamová M. 1999: Tephrostratigraphy of the Neogene volcaniclastics (Moravia, Lower Austria, Poland). *Geol. Carpath*. 50, Spec. Iss. 126–128.

Nehyba S., Petrová-Tomanová P. & Zágoršek K. 2008: Sedimentological and palaeocological records of the evolution of the south-western part of the Carpathian Foredeep (Czech Republic) during the Early Badenian. *Geol. Quarterly* 52, 1, 45–60.

Nehyba S., Roetzel R. & Maštera L. 2012: Provenance analysis of the Permo-Carboniferous fluvial sandstones of the southern part of the Boskovice Basin and the Zöbing Area (Czech Republic, Austria): implications for paleogeographical reconstructions of the post-Variscan collapse basins. *Geol. Carpath.* 63, 5, 365–382.

Nehyba S., Holcová K., Gedl P. & Doláková N. 2016: The Lower Badenian transgressive-regressive cycles – a case study from Oslavany (Carpathian Foredeep, Czech Republic). *Neues Jahrb. Geol. Paläontol.* 279, 2, 209–238.

Nehyba S., Hanáček M., Engel Z. & Stachoň Z. 2017: Rise and fall of a small ice-dammed lake - Role of deglaciation processes and morphology. *Geomorphology* 295, 662–679.

Nemec W. 1990a: Deltas — remarks on terminology and classification. In: Colella A. & Prior D.B. (Eds.): Coarse-Grained Deltas. *IAS Spec. Publ.* 10, 3–12.

Nemec W. 1990b: Aspects of sediment movement on steep delta slopes. In: Colella A. & Prior D.B. (Eds.): Coarse-Grained Deltas. *IAS Spec. Publ*. 10, 29–74.

Nemec W. 1995: The dynamics of deltaic suspension plumes. In: Oti M.N. & Postma G. (Eds.): Geology of Deltas. *Balkema*, Rotterdam, 31–93.

Nemec W., Lønne I. & Blikra L.H. 1999: The Kregnes moraine in Gauldalen, west-central Norway: anatomy of a Younger Dryas proglacial delta in a palaeofjord basin. *Boreas* 28, 454–476.

Novák Z. 1985: Litologická charakteristika sedimentů miocénu na mapovém listu Pouzdřany /34-124/. *MS ČGS.*

Novák Z. 1986a: Litologická charakteristika sedimentů miocénu na mapovém listu Mikulov /34-142/. *MS ČGS.*

Novák Z. 1986b: Litologická charakteristika sedimentů miocénu na mapovém listu 1: 25 000 Pohořelice /34-122/. *MS ČGS.*

Otava J. 1998: Trends of changes in the composition of siliciclastics of the Lower Carboniferous at Drahany Upland (Moravia) and their geotectonic interpretation. *Geol. výzk. Mor. Slez. v r. 1997,* 62–64 (in Czech).

Otava J., Krejčí O. & Sulovský P. 1997: First results of electron microprobe analyses of detrital garnets from the Rača Unit of the Magura Group. *Geol. výzk. Mor. Slez. v r. 1996,* 39–42 (in Czech).

Otava J., Sulovský P. & Čopjaková R. 2000: Provenance changes of the Drahany Culm greywackes: statistical evaluation. *Geol. Výzk. Mor. Slez. v r. 1999*, 94–98 (in Czech).

Petrová P. 2002: The results of study of the intraklasts (micropaleontology) at the locality Troskotovice. *Geol. výzk. Mor. Slez. v r. 2001*, 40–42 (in Czech).

Plink-Björklund P. & Ronnert L. 1999: Depositional processes and internal architecture of Late Weichselian ice-margin submarine fan and delta settings, Swedish west coast. *Sedimentology* 46, 215–234.

Postma G. 1990: Depositional architecture and facies of river and fan deltas: a synthesis. In: Colella A. & Prior D.B. (Eds.): Coarse-Grained Deltas. *IAS Spec. Publ*. 10, 13–27.

Postma G. & Cruickshunk C. 1988: Sedimentology of a late Weichselian to Holocene terraced fan delta, Varangerfjord, norhern Norway. In: Nemec W. & Steel R. (Eds.): Fand Deltas: Sedimentology and Tectonic Settings. *Blackie*, London, 144–157.

Postma G. & Roep T.B. 1985: Resedimented conglomerates in the bottomsets of Gilbert-type gravel deltas. *J. Sediment. Res*. 55, 874–885.

Postma G., Nemec W. & Kleinspehn K.I. 1988: Large floating clasts in turbidites: a mechanism for their emplacement. *Sediment. Geol*. 58, 1, 47–61.

Powers M.C. 1953: A new roundness scale for sedimentary particles. *J. Sediment. Petrol*. 23, 117–119.

Přichystal A. 2009: Petrographical analysis of pebbles from Mušov. In: Valoch K. (Ed.): Mušov I (county Břeclav) — Geological and archeological locality on southern Moravia. *Studies in Anthropology, palaeoethology, palaeontology and Quaternary Geology* 30, 189–93 (in Czech with English abstract).

Řehánek J. 2001: Microscopical analysis of thin sections. *MS Archive ÚGV PřF MU*, 1–4 (in Czech).

Rhine J.L. & Smith D.G. 1988: The late Pleistocene Athabasca braid delta of northeastern Alberta, Canada: a paraglacial drainage system affected by aeolian sand supply. In Nemec W. & Steel R.J. (Eds.): Fan Deltas: Sedimentology and Tectonic Settings. *Blackie and Son*, 158-169.

Roberts M.C., Niller H.-P. & Helmstetter N. 2003: Sedimentary architecture and radar facies of a fan delta, Cypress Creek, West Vancouver, British Columbia. In: Bristow C.S. & Jol H.M. (Eds.): Ground Penetrating Radar in Sediments. *The Geological Society London*, Bath, 111–126.

Sarkisjan S.G. & Klimova L.T. 1955: Orientation of the pebbles and methods of their study for paleogeographic constructions. *AN SSSR*, Leningrad, 1–44 (in Russian).

Shanley K.W. & McCabe P.J. 1994: Perspectives on the sequence stratigraphy of continental strata. *AAPG Bull.* 78, 544–568.

Shukla U.K., Singh I.B., Sharma M. & Sharma S. 2001: A model of alluvial megafan sedimentation: Ganga Megafan. *Sediment. Geol*. 144, 243–262.

Sneed E.D. & Folk R.L. 1958: Pebbles in the lower colorado River, Texas: a stud in particle morphogenesis. *J. Geol*. 66, 114–150.

Sohn Y.K., Kim S.B., Hwang I.G., Bahk J.J., Choe M.Y. & Chough S.K. 1997: Characteristics and depositional processes of large–scale gravelly Gilbert–type foresets in the Miocene Dousman fan delta, Pohang basin, SE Korea. *J. Sediment. Res*. 67, 130–141.

Sohn Y.K., Rhee C.W. & Shon H. 2001: Revised stratigraphy and reinterpretation of the Miocenew Pohang basinfill, SE Korea: sequence development in response to tectonism and eustasy in a back-arc basin margin. *Sediment. Geol.* 143, 265–285.

Stráník Z., Čtyroký P. & Havlíček P. 1999: The geological history of the Palava Hill. *Sborník Geologických věd, Geologie* 49, 5–32 (in Czech).

Stráník Z., Hrouda F., Otava J., Gilíková H. & Švábenická L. 2007: The Upper Oligocene-Lower Miocene Krosno lithofacies in the Carpathian Flysch Belt (Czech Republic): sedimentology, provenance and magnetic fabrics. *Geol. Carpath.* 58, 4, 321–332.

Švábenická L. & Čtyroká J. 1999: Biostratigraphic correlation (foraminifers and nannofosils) of the Karpathian and Lower Badenian sediments in the Alpine-Carpathian Foredeep (Moravia and Lower Austria). *Biuletyn PIG* 387, 187–189.

Tomanová-Petrová P. & Švábenická L. 2007: Lower Badenian biostratigraphy and paleoecology: a case study from the Carpathian Foredeep (Czech Republic). *Geol. Carpath.* 58, 333–352.

Triebold S., Eynatten H. von, Luvizotto G.L. & Zack T. 2007: Deducing source rock lithology from detrital rutile geochemistry: An example from the Erzgebirge, Germany. *Chem. Geol*. 244, 421–436.

Triebold S., Eynatten H. von & Zack T. 2012: A recipe for the use of rutile in sedimentary provenance analysis. *Sediment. Geol*. 282, 268–275.

Tucker M. (Ed.) 1988: Techniques in Sedimentology. *Blackwell Science*, Oxford, 1–394.

von Eynatten H. & Gaupp R. 1999: Provenance of Cretaceous synorogenic sandstones in the Eastern Alps: constraints from framework petrography, heavy mineral analysis and mineral chemistry. *Sediment. Geol*. 124, 81–111.

Walker R.G . & James N.P. 1992: Facies Models: Response to Sea Level Changes. *Geological Association of Canada*, St. John's, 1–380.

Weissmann G.S., Hartley A.J., Nichols G.J., Scuderi L.A., Olson M., Buehler H. & Banteah R. 2010: Fluvial form in modern continental sedimentary basins: distributive fluvial systems. *Geology* 38, 39–42.

Zack T., von Eynatten H. & Kronz A. 2004a: Rutile geochemistry and its potential use in quantitative provenance studies. *Sediment. Geol*. 171, 37–58.

Zack T., Moraes R. & Kronz A. 2004b: Temperature dependence of Zr in rutile: empirical calibration of a rutile thermometer. *Contrib. Mineral. Petrol*. 148, 471–488.

Zaitlin B.A., Dalrymple R.W. & Boyd R. 1994: The stratigraphic organization of incised-valley system associated with relative sea-level change. In: Dalrymple R.W., Boyd R. & Zaitlin B.A. (Eds.): Incised-Valley Systems: Origin and Sedimentary Sequences. *SEPM Spec. Publ.* 51, 45-60.

Zingg Th. 1935: Beiträge zur Schotteranalyse. *Miner. Petrogr. Mitt. Schweiz*. 15, 39–140.